# Description of the real time PWR power plant model PWR-PLASIM

**Forskningscenter Risø, Roskilde**

*Publication date:*
1974

*Document Version*
Publisher's PDF, also known as Version of record

Risø Report No. 318

Risø Report No. 318

Danish Atomic Energy Commission

Research Establishment Risø

# Description of the Real Time PWR Power Plant Model PWR-PLASIM

*by* P. la Cour Christensen

November 1974

*Sales distributors:* Jul. Gjellerup, 87, Sølvgade, DK-1307 Copenhagen K, Denmark

*Available on exchange from:* Library, Danish Atomic Energy Commission, Risø, DK-4000 Roskilde, Denmark

INIS Descriptors

HYBRID COMPUTERS
NUCLEAR POWER PLANTS
PRESSURIZERS
PWR TYPE REACTORS
REACTOR SIMULATORS
REAL TIME SYSTEMS
SIMULATION
STEAM GENERATORS
STEAM TURBINES

UDC 621.039.524.4-98 : 681.3 : 519.283

November 1974

Risø Report No. 318

# Description of the Real Time PWR Power Plant Model PWR-PLASIM

by

P. la Cour Christensen

Danish Atomic Energy Commission
Research Establishment Risø
Department of Reactor Technology

## Abstract

A description is given of a PWR power plant model working in real time on a hybrid computer. The basic equations are derived and simplifications discussed. Independent, detailed models were prepared for the steam generator, the pressuriser and the reactor fuel and used in the development of simpler models. The independent, detailed models are included in the presentation.

ISBN 87 550 0303 6

## CONTENTS

# 1. INTRODUCTION

A PWR power station model including the major components in both primary and secondary circuits was developed as a tool for investigating the dynamic characteristics of the complete station. Investigations comprise the analysis of control systems, of normal operation procedures in the power range 25-100% of full load, and of some accidents of a minor nature.

The model is implemented on a hybrid computer in order to achieve computation in real time with the best man-machine communication available at Risø. The price paid for these advantages is limited computing power, which results in limits to the complexity of the model.

As the structure and details of the model depend heavily on the computer configuration, this is given in Appendix A.

The power station model is composed of submodels of the following units: the reactor, the primary circulation circuit, the pressuriser, one steam generator, and on the secondary side a turbine with a reheater between the high and low pressure section. The station is coupled to an electrical power grid including a further generating unit represented in a very simple way. The computer system only gives space for one steam generator, and no space at all for the condenser and the feedwater reheaters on the secondary side. It is regarded as more important to save equipment and computing time for simulation of a control system for the power plant.

A diagram showing the basic physical system is given in fig. 1, and a diagram of the structure of the model is given in fig. 2.

Some of the components have been studied separately by independent models, most extensively the steam generator and the pressuriser. These models were used to develop more simplified models for the complete station model. They may, in addition, be used for a detailed study of transient effects in the individual components, when input transient time functions have been calculated by the station model.

The most detailed submodel is the reactor model, which is developed in one space dimension along the fuel elements. All quantities across the core are taken as mean values. The space axis is divided into 16 sections (14 fuel and 2 reflector sections) for the neutron kinetic calculations and 14 sections for the heat transfer calculations. The kinetic calculations are carried out by a digital routine, whereas the heat transfer calculations are performed as hybrid computations. This procedure gives optimum utilisation of the computer concerning computing speed, equipment, accuracy and stability.

The heat transmission and the temperature distribution in the fuel may be studied in more detail by an independent Fortran program, where the fuel pellets are divided into ten shell segments and one canning segment. The program runs in real time synchronized from the analog computer. It outputs some variables via DA converters for registration.

The independent steam generator model is a one-dimensional model of a U-tube type with 40 sections along the U-tubes. It is implemented by a Fortran program and does not work in a fixed time scale as the computing speed is slow, about 20 times slower than real time. In the simplified version of the station model the 40 sections are lumped together in one section described by appropriately selected weighting functions. This version is carried out by analog components with a few temperature-dependent parameters calculated by a digitial routine.

The pressuriser was studied extensively by an independent model consisting of equations for a two-point system: the water and the steam phase. Each phase may exist in one of the two states: saturated and non-saturated (superheated steam and subsaturated water). The influence of different effects such as transition between saturation and non-saturation and heat transmission to the tank wall was studied. A slightly simplified version is used for the station model. The independent model is programmed for the digital machine in a macro-assembler language. It runs in either real time or ten times faster synchronized from the analog machine with outputs via DA converters only. The simplified version is carried out as a digital routine.

The primary circulation circuit is modelled as one single loop since only one steam generator is included. It is described by compartment equations using eight compartments for the circulation line, four for the steam generator and four for the reactor outside the core. The pump is not modelled as it normally runs at constant speed. The calculations are programmed as a digital routine.

The steam load system consists of a turbine which for simulation is divided into HP and LP sections, regulating valve, and reheater with moisture separator. The pressure profile and the reheater steam temperature are calculated by analog components, while the turbine power is calculated in a digital routine using a Mollier diagram.

The electrical grid is simulated quite simply by a time lag function giving the frequency deviations for production - demand power mismatch. All other production units are combined in one unit with power-frequency control. The PWR station may be equipped with a power or a power-frequency control system.



The digital routines are written in a macro-assembler language developed only for hybrid calculations. This makes it possible to use the PDP8 central unit, the floating point processor and the EAI analog computer for simultaneous calculations. By careful distribution of the tasks among the 3 units, it is possible to run the simulation in real time with a time step of 0.1 sec for the digital and hybrid routines. Some few milliseconds of the 100 ms time step and some analog components are in reserve for control system simulation. The diagram in fig. 3 shows how the computations are distributed in time on the three computing units.

The following chapters give the basic equations for both the station submodels and the independent models of separate units. The equations contain several temperature- and pressure-dependent parameters for heat transfer and friction calculations. They are normally approximated by polynomials or calculated by diode function generators. In a few cases some parameters are assembled in a single function for simplification, and only for these cases are numerical values given for justification in this report. A following report[1] will give the numerical values for a test example, the equations with numerical values, scaled equations and patching diagrams for the analog computer, and program printouts.

In the basic version the model has three main input variables: control rod position, boron acid concentration and electrical power load. The three control input variables - feed water flow to the steam generator, coolant flow and heating power for the pressuriser - are given by local control algorithms that must be included for stability reasons. The control parameters, however, are easily changed. An overall power control system is not included as the model is intended for use in a study of different control methods.

Perturbation of variables and parameters, which are fixed for normal operation, is possible, but for the basic version requires acquaintance with details in the program. For specific purposes some few perturbation possibilities may be included in a special version.

## 2. NEUTRON KINETICS

The neutron kinetics is described by the one-dimensional, one-group diffusion equation:

$$\frac{1}{v}\frac{\partial \varphi}{\partial t} = D\frac{\partial^2 \varphi}{\partial x^2} - \Sigma_a \varphi + (1-\beta)\nu\Sigma_f \varphi + \sum_i \lambda_i C_i \,. \qquad (2.1)$$

The parameters D, $\Sigma_a$ and $\nu\Sigma_f$ are all functions of the core composition and the temperature of the different components. Static reactor physics calculations have been used to find second-order polynomials in five variables for the three parameters. The five variables are: fuel temperature, water temperature, water density, boron acid concentration and control rod density.

As the equations are solved by a digital routine, a sampling in time is necessary. A sampling time equal to 0.1 sec is chosen according to the thermal and hydraulic time constants and the delayed neutron decay constants. This time step is much larger than the time constant for the diffusion equation, so any transient in the flux, for a fixed perturbation in the neutron parameters, will die out completely in one time step. It means that the derivative term on the left side may be neglected.

Integration in space is carried out by division of the space axis in segments $\Delta x$ and transformation to a difference equation by first-order differences:

$$\frac{d^2\varphi}{dx^2} = \frac{1}{\Delta x^2}(\varphi_{j-1} - 2\varphi_j + \varphi_{j+1}). \qquad (2.2)$$

This corresponds to the assumption that the flux values for three neighbouring sections are placed on a second-order curve, when the flux $\varphi_j$ refers to the middle of section number j.

The boundary value problem is solved by means of reflector sections at each end of the fuel sections. It is assumed that the neutron current J back to the reflector from the surroundings is equal to zero. For the lower section at $x = 0$ it means that:

$$J_+ = \frac{1}{4}(\varphi_o - 2D(\frac{d\varphi}{dx})_o) = 0 \qquad \text{giving} \qquad (2.3)$$

$$(\frac{d\varphi}{dx})_o = \frac{\varphi_o}{2D}. \qquad (2.4)$$

We can now use an approximation corresponding to the linear difference approximation for the fuel sections and assume that the fluxes $\varphi_o$, $\varphi_1$ and $\varphi_2$ belong to a second-order curve. $\varphi_1$ and $\varphi_2$ are the fluxes in the middle of the reflector section and the first fuel section, and $\varphi_o$ the flux at the reflector boundary. This gives an expression for the flux slope at $x = 0$:



$$(\frac{d\varphi}{dx})_o = \frac{9\varphi_1 - \varphi_2}{3\Delta x + 16D}. \qquad (2.5)$$

where D is the diffusion constant for the reflector section.

Similarily we obtain an expression for $\frac{d\varphi}{dx}$ at the other reflector boundary:

$$(\frac{d\varphi}{dx})_{m+1} = -\frac{9\varphi_m - \varphi_{m+1}}{3\Delta x + 16D}, \qquad (2.6)$$

where m is the total number of sections including the two reflector sections.

Insertion of (2.2), (2.5) and (2.6) into the diffusion equation (2.1) gives:

$$C_{j,j-1}\,\varphi_{j-1} + C_{j,j}\,\varphi_j + C_{j,j+1}\,\varphi_{j+1} = (-\sum_i \lambda_i C_i)_j, \qquad (2.7)$$

which can be written as a matrix equation

$$\{C\}\,\varphi = S, \qquad (2.8)$$

where S is a source vector and $\{C\}$ is a band matrix with

$$C_{j,j} = (1-\beta)\,\nu\Sigma_f - \Sigma_a - \frac{2D}{\Delta x^2}$$

$$C_{j,j-1} = C_{j,j+1} = \frac{D}{\Delta x^2}$$

for $2 \leq j \leq m-1$

$$C_{1,1} = C_{m,m} = -(\Sigma_a + \frac{D}{\Delta x}(\frac{1}{\Delta x} + \frac{9}{3\Delta x + 16D}))$$

$$C_{1,2} = C_{m,m-1} = \frac{D}{\Delta x}(\frac{1}{\Delta x} + \frac{1}{3\Delta x + 16D})$$

for the first and last row in (2.8).

The solution of the diffusion equation is thus reduced to the solution of n linear equations with coupling coefficients different from zero only for neighbouring elements. The coefficients in the matrix C have to be calculated for each time step as functions of five variables, as mentioned earlier, with values corresponding to the previous time step. It means that a time delay of half a time step is introduced in the kinetic feedback

loop. With a time step of 100 mS, the delay of 50 mS is negligible compared with the thermal time constant.

The neutron flux is converted to power according to the equation:

$$N = \frac{A}{\nu} V_f \nu \Sigma_f \varphi, \qquad (2.9)$$

where N is the neutron power per core section, A is the energy release per fission, and $V_f$ is the core volume per section.

The source term in equation (2.7) is the delayed netrons for which we use three groups. The concentration of the emitters is calculated according to the equation:

$$\dot{C}_i = -\lambda_i C_i + \beta_i \nu \Sigma_f \varphi, \qquad (2.10)$$

for each group in each core section. For the present version of the model it means that (2.10) must be solved 3 x 14 times for each time step. This is best done by a digital routine involving sampling in time. Equation (2.10) is integrated using the difference equation:

$$\frac{1}{\Delta t}(C_{n+1} - C_n) = -\frac{\lambda}{2}(C_{n+1} + C_n) + \beta \nu \Sigma_f \varphi_n, \qquad (2.11)$$

which can be reduced to the following form:

$$C_{n+1} = \frac{2-\lambda\Delta t}{2+\lambda\Delta t}(C_n + \frac{2\beta\Delta t}{2-\lambda\Delta t} \nu \Sigma_f \varphi_n). \qquad (2.12)$$

Neutron kinetic symbols

| | | |
|---|---|---|
| $\varphi$ | : Neutron flux | $1/cm^2 s$ |
| D | : Diffusion constant | cm |
| $\Sigma_a$ | : Absorbtion cross section | 1/cm |
| $\Sigma_f$ | : Fission cross section | 1/cm |
| v | : Thermal neutron mean velocity | cm/s |
| $\nu$ | : Yield of prompt neutrons per fission | |
| $C_i$ | : Concentration of delayed neutron emitter group i | $1/cm^3$ |
| $\lambda_i$ | : Decay constant for delayed neutron emitter group i | 1/s |



| | | |
|---|---|---|
| $\beta_i$ | : Yield of delayed neutrons group i | |
| A | : Energy release per fission | MJ |
| $V_f$ | : Core volume per core section | $m^3$ |
| $\Delta x$ | : Length of core section | m |
| N | : Nuclear power per core section | MW |
| $\Delta t$ | : Time step | sec |

## 3. THE FUEL MODEL

The fuel is divided into vertical sections along the coolant flow, as mentioned in chapter 2. The nuclear power is used with an even distribution over the cross section, and the axial temperature profile is taken as constant within each section. The fuel model for the complete station model is a simple point model, but the validity has been checked by comparison with a more detailed model with ten-shell sections around the axis of the fuel pin. Section 3.1 gives a description of the ten-shell section model and 3.2 of the simple point model.

### 3.1. A Ten-shell Section Fuel Model

The fuel pin is divided into ten cylindrical sections with equal thickness. The heat transmission is calculated with a temperature-dependent heat transfer coefficient, but constant specific heat for the fuel. Both these quantities are taken as constants for the canning, and also the heat transfer coefficient for the air gap is used as a constant. The heat transfer from the canning surface to the coolant is calculated according to the equation (3.1.1) derived from the Dittus-Boelter equation.

$$k_{cac} = \frac{0.023\ E\text{-}3}{De_c^{0.2}} O_{ca} H_c(T_c) \left(\frac{W_c}{A_c}\right)^{0.8} \qquad (3.1.1)$$

where

$$H_c(T_c) = \frac{C_p^{0.3} \lambda^{0.7}}{\eta^{0.5}}$$

is taken as a function of the coolant temperature only, as the pressure dependence is extremely small. $H_c(T)$ is plotted in fig. 4, which shows that a linear approximation can be used.

The temperatures in the shell sections and in the canning are calculated by the heat balance equations:

$$C_1\dot{T}_1 = Q_1 - k_1(T_1 - T_2)$$

$$C_j\dot{T}_j = Q_j + k_{j-1}(T_{j-1} - T_j) - k_j(T_j - T_{j+1}) \qquad (3.1.2)$$

$$C_{11}\dot{T}_{11} = k_{10}(T_{10} - T_{11}) - k_{11}(T_{11} - T_c),$$

where $1 \leq j \leq 10$ refers to fuel sections and $j = 11$ refers to the canning. The coefficients are given by the following set of equations:

$$C_j = \frac{2j-1}{100} C_u \qquad \text{for } 1 \leq j \leq 10$$

$$Q_j = \frac{2j-1}{100} N \qquad \text{for } 1 \leq j \leq 10$$

$$C_{11} = C_{ca} \qquad (3.1.3)$$

$$k_j = (2\pi \lambda_{j,j+1} / \ln \frac{2j+1}{2j-1}) \Delta x M_u \qquad \text{for } 1 \leq j \leq 9$$

$$\frac{1}{k_{10}} = Z_{ugca} = (\frac{\ln(20/19)}{2\pi \lambda_{10,g}}) + \frac{1}{k_g} + \frac{\Delta r_{ca}}{H_{ca} \lambda_{ca}}) \frac{1}{\Delta x M_u}$$

$$k_{11} = \frac{0.023\,E\text{-}3}{De_c^{0.2}} O_{ca} H_c(T_c) (\frac{W_c}{A_c})^{0.8}$$

$$\lambda_{j,j+1} = f_\lambda(\frac{1}{2}(T_j + T_{j+1}))$$

$$\lambda_{10,g} = f_\lambda(\frac{1}{2}(T_{10} + T_{ug}))$$

$$T_{ug} = Z_{gca} k_{10}(T_{10} - T_{11}) + T_{11}$$

$$Z_{gca} = (\frac{1}{k_g} + \frac{\Delta r_{ca}}{H_{ca} \lambda_{ca}}) \frac{1}{\Delta x M_u}$$

$$H_{ca} = \pi(2 r_u + 2 \Delta r_g + \Delta r_{ca}).$$



The heat is distributed among the fuel sections assuming an even distribution over the fuel cross section. $C_j$ is the heat capacity of the shell sections; $k_j$ is the heat transfer coefficient between the sections. $k_{10}$ is composed of the heat resistance in the half part of the outmost fuel shell, the air gap and the whole canning; $k_{11}$ is the heat transfer coefficient from the canning surface to the coolant. It means that the heat capacity of the canning, $C_{11}$, is located at the canning surface.

The equations (3.1.2) are solved by a digital program with the difference approximation:

$$\frac{C_j}{\Delta t}(T_{j,n+1} - T_{j,n}) = Q_j + k_{j-1}(T_{j-1} - T_j)_{n+1} + k_j(T_j - T_{j+1})_{n+1}. \qquad (3.1.4)$$

The equations can then be rearranged to a system of linear equations:

$$(\frac{C_1}{\Delta t} + k_1) T_{1,n+1} - k_1 T_{2,n+1} = Q_1 + \frac{C_1}{\Delta t} T_{1,n}$$

$$-k_{j-1} T_{j-1,n+1} + (\frac{C_j}{\Delta t} + k_{j-1} + k_j) T_{j,n+1} - k_j T_{j+1,n+1} = Q_j + \frac{C_j}{\Delta t} T_{j,n}$$

(3.1.5)

$$-k_{10} T_{10,n+1} + (\frac{C_{11}}{\Delta t} + k_{10} + k_{11}) T_{11,n+1} = k_{11} T_c + \frac{C_{11}}{\Delta t} T_{11,n}$$

which can also be written as a matrix equation with the band matrix $\{K\}$:

$$\{K\} T_{n+1} = Q + C \cdot T_n . \qquad (3.1.6)$$

## 3.2. A Two-point Fuel Model

In the point model the fuel is combined in one section surrounded by the canning as another section with an air gap between. Comparison of transients for the two models has shown that reasonably good agreement can be obtained with selection of the heat transfer coefficient for the fuel from a static calculation.

The two-point model is described by the following set of equations:

$$C_u \dot{T}_u = N - k_f(T_u - T_{ca})$$

$$C_{ca} \dot{T}_{ca} = k_f(T_u - T_{ca}) - Q_c$$

$$\frac{1}{k_f} = Z_{ugca} = \frac{K_u}{\lambda_u} + Z_{gca}$$

$$Z_{gca} = \left(\frac{1}{k_g} + \frac{\Delta r_{ca}}{\lambda_{ca} H_{ca}}\right) \frac{1}{\Delta x \, M_u} \qquad (3.2.1)$$

$$T_{ug} = T_{ca} + Z_{gca} \, k_f(T_u - T_{ca})$$

$$\lambda_u = f_\lambda\left(\frac{1}{2}(T_u + T_{ug})\right)$$

$$Q_u = k_f(T_u - T_{ca}) .$$

The coefficient $K_u$ is chosen so that the fuel temperature $T_u$ is equal to the fuel mean temperature for the ten-section model at 300 W/cm fuel pin (corresponding to approximately 250 MW per core section in the actual study). Calculation of the heat flow $Q_c$ to the coolant is discussed in the next chapter.

The precision of the model is illustrated in fig. 5, which shows a transient in heat flow for the two-point model and the ten-section model for a step in section power from 125 to 250 MW. The agreement is found to be extremely good considering the great difference in number of fuel segments.

As the equations (3.2.1) are used in a discrete time model, the two differential equations must be converted to difference equations. Even though the driving variable N is only known at time n for calculation of temperatures at time (n + 1), the internal feedbacks will be calculated for time $(n + \frac{1}{2})$ to improve the stability. The two differential equations will be solved as follows:

$$T_u(n+1) = T_u(n) + \Delta_t T_u$$

$$\Delta_t T_u = \frac{\Delta t}{C_u} \left(N(n) - k_f(T_u(n + \tfrac{1}{2}) - T_{ca}(n + \tfrac{1}{2}))\right)$$

$$T_{ca}(n+1) = T_{ca}(n) + \Delta_t T_{ca} \qquad (3.2.2)$$

$$\Delta_t T_{ca} = \frac{\Delta t}{C_{ca}} \left(k_f(T_u(n+\tfrac{1}{2}) - T_{ca}(n + \tfrac{1}{2})) - Q_c(n+\tfrac{1}{2})\right).$$



Fuel model symbols

| | | | |
|---|---|---|---|
| $r_u$ | : | Radius of fuel pellets | m |
| $\Delta r_g$ | : | Air gap between fuel pellets and canning | m |
| $\Delta r_{ca}$ | : | Thickness of canning | m |
| $De_c$ | : | Hydraulic diameter of the cooling channel | m |
| $\Delta x$ | : | Length of a fuel section | m |
| $M_u$ | : | Number of fuel pins in core | m |
| $H_{ca}$ | : | Canning heat transfer area per m fuel pin | $m^2/m$ |
| $O_{ca}$ | : | Canning surface per core section | $m^2$ |
| $C_u$ | : | Heat capacity of fuel per core section | $MJ/^oC$ |
| $C_j$ | : | Heat capacity of fuel in section number j | $MJ/^oC$ |
| $k_j$ | : | Heat transfer coefficient from fuel section number j to j+1 | $MW/^oC$ |
| $k_g$ | : | Heat transfer coefficient for the air gap per m fuel pin | $MW/^oC$ m |
| $\lambda$ | : | Thermal conductivity | $MW/^oC$ m |
| $\lambda_{j,j+1}$ | : | Thermal conductivity from fuel section j to j+1 | $MW/^oC$ m |
| $\lambda_{10,g}$ | : | Thermal conductivity for outer half of the outmost fuel section | $MW/^oC$ m |
| $\lambda_{ca}$ | : | Thermal conductivity for canning | $MW/^oC$ m |
| $Z_{gca}$ | : | Thermal resistance in air gap and canning | $^oC/MW$ |
| $Z_{ugca}$ | : | Thermal resistance in air gap, canning and outer half of outmost fuel section | $^oC/MW$ |
| $Q_j$ | : | Heat released in fuel section j | MW |
| $T_j$ | : | Temperature in fuel section j | $^oC$ |
| $T_{ug}$ | : | Temperature of fuel pellet surface | $^oC$ |
| $T_u$ | : | Mean temperature of fuel pellets | $^oC$ |
| $T_{ca}$ | : | Canning temperature | $^oC$ |
| $W_c$ | : | Coolant flow | kg/s |

# 4. THE PRIMARY CIRCUIT WITH HEAT TRANSPORT AND BORON ACID DISTRIBUTION

## 4.1. Heat Transfer in Core

The temperature rise of the coolant in the reactor core is calculated by the energy balance equation assuming an even distribution of flow velocity over the cross section. The basic form of the equation is:

$$W_c\, c_p \frac{\partial T_c}{\partial x} = q_t - A_c \rho_f\, c_p \dot{T}_c . \qquad (4.1)$$

The equation is solved in discrete spaces to discrete times. The core is divided into 14 sections along the flow direction as mentioned in chapter 2. The space derivative for section j is approximated by the difference term:

$$\frac{\partial T_c}{\partial x} = \frac{1}{\Delta x}\,(T_c(j) - T_c(j-1)). \qquad (4.2)$$

The time derivative to time step n is approximated by the difference term:

$$\frac{\partial T_c}{\partial t} = \frac{1}{\Delta t}\,(T_c(n+1) - T_c(n)) \qquad (4.3)$$

Equation (4.1) can then be written as:

$$T_c(j, n+1) = T_c(j-1, n+1) + \frac{1}{W_c}\left(\frac{Q_t(j)}{c_p} - \frac{V_c \rho_f}{\Delta t}\,\Delta_t T_c(j, n+1)\right)$$

$$\Delta_t\, T_c(j, n+1) = T_c(j, n+1) - T_c(j, n). \qquad (4.4)$$

The actual values for the core geometry and the mass flow rate give a ratio of mass flow to section mass contents equal to approximately 2:1, which is about twice the stability limit for simple Euler integration. But due to the internal feedback in equation (4.4), we do get a stable solution. Further, the dynamic accuracy is sufficient, as the input variable $Q_t$ for the equation is smoothed by the heat capacity in the fuel.

The heat flow from the fuel is calculated according to either the Dittus Boelter or the Thom relation, depending on which of them gives the greatest heat flow. The calculations are done in parallel and the highest value is chosen. The equations are:



$$Q_{c1} = \frac{0.023\ \text{E-3}}{De_c^{0.2}}\, O_{ca}\, \left(\frac{W_c}{A_c}\right)^{0.8} H_c\,(T_c)\,(T_{ca} - T_c)\,. \qquad (4.5)$$

$$Q_{c2} = 1.973\ \text{E-3}\ \ O_{ca} \exp\left(\frac{p_p}{43.4}\right)(T_{ca} - T_{ps})^2. \qquad (4.6)$$

For the normal power range, the heat transfer will be governed by equation (4.5), but for transients with high values of the nuclear power equation (4.6) will determine the heat flow and set a rather sharp limit for the canning temperature due to the quadratic term in the temperature difference.

For the temperature range 275 to 325°C, the heat transfer parameter $H_c(T_c)$, discussed in chapter 3, will vary about $\pm$ 2%, so it may be used as a constant.

The temperature margin against boiling is about 25°C for full power, but even so a few steam bubbles are produced. These are without significance in the normal power range, but may have influence on high power transients, so a rough calculation of the void contents and the mean coolant density is included.

The void calculation is based upon an empirical function giving the relative power producing steam. It is taken as a function of the temperature difference $(T_{ps} - T_c)$ only, and evaluated from static calculations using a more refined void calculation. The boiling power and the power for water heating is expressed as:

$$Q_b = Q_c\, f_v\,(T_{ps} - T_c)$$

$$Q_t = Q_c - Q_b\,, \qquad (4.7)$$

where $f_v(T_{ps} - T_c)$ is the empirical function mentioned above.

The further calculation of the void contents is based upon the assumption that the steam bubbles are released from the canning surface and carried along with the water without condensing. This assumption is justified by the high water velocity, which gives a mean transfer time of 0.7 sec for the core.

The basic equation for the void calculation is the mass continuity equation:

$$v_c\, A_c \frac{\partial a}{\partial x} = \frac{q_b}{h_{fg}\, \rho_{gs}} - A_c \dot{a}\,. \qquad (4.8)$$

It is solved in the same way as equation (4.1) giving:

$$\alpha(j, n+1) = \alpha(j-1, n+1) + \frac{\rho_f}{W_c}\left(\frac{Q_b(j)}{h_{fg}\rho_{gs}} - \frac{V_c}{\Delta t}\Delta_t \alpha(j, n+1)\right)$$

$$\Delta_t \alpha(j, n+1) = \alpha(j, n+1) - \alpha(j, n)\,. \qquad (4.9)$$

For the actual study we do use constant values of $h_{fg}$, $\rho_{gs}$ and $\rho_f$, as variation in these parameters is only a second-order effect in a second-order variable.

The mean coolant density is calculated as:

$$\rho_m = \rho_f - \alpha(\rho_f - \rho_{gs})\,, \qquad (4.10)$$

where $(\rho_f - \rho_{gs})$ is taken as a constant while $\rho_f$ is a function of $T_c$.

The steam leaving the core is mixed completely with the water in the upper plenum of the reactor tank, and condenses due to the relatively low water velocity (the transit time is about 2.5 sec). In the model the condensation is removed to a compartment close to the core with the same geometry as the core sections (identical to the upper reflector for the kinetic calculations). The calculations for an extra core section are repeated with $Q_b = 0$ and $Q_t$ equal to the sum of $Q_b$ for the 14 core sections.

The heat transfer calculations for both fuel and coolant, which are described by the equations (3.2.1), (4.4) - (4.7) and (4.9) - (4.10), are implemented as pure hybrid calculations. The equations are solved as algebraic equations by analog equipment with input values from the digital computer, which again reads the output values and updates the profiles stored as arrays. The main advantage of the hybrid procedure is the high calculation speed, but also a more stable and accurate solution is obtained than by pure digital calculation due to the internal feedback from the cross couplings in the equations.

## 4.2. Heat Transport in the Primary Circuit

The temperature distribution in the primary loop is calculated with a division of the loop into compartments as shown in fig. 6. The four core compartments are only used for calculation of boron acid concentration, as discussed later. The circulation tubes are divided into relatively small compartments to get a reasonable approximation of the combined time delay and mixture process. The reason for selecting only two compartments for



the steam generator U-tubes is given in chapter 6.

The calculation for the individual compartments follows the equation:

$$T(o, n+1) = (T(o, n) + \frac{\Delta t W}{V \rho_f}\ T(i, n+1))/(1 + \frac{\Delta t W}{V \rho_f}). \qquad (4.11)$$

This is actually the same equation as (4.4) without the heat transfer term Q.

The net mass flow from the individual compartments due to thermal expansion is calculated together with the temperature distribution. The equation is:

$$\dot{m} = -V\dot{\rho} = -V\frac{d\rho_f}{dT}\dot{T} = \frac{d\rho_f}{dT}\ \frac{W}{\rho_f}(T(o, n+1) - T(i, n+1))\,. \qquad (4.12)$$

The same term for mass flow from the core is calculated as:

$$\dot{m} = -V\frac{d\rho_f}{dT}\ \frac{1}{\Delta t}\ \sum_j \Delta_t T_c(j, n)\,, \qquad (4.13)$$

where the sum is calculated in the hybrid routine for the core.

The temperature distribution and the total expansion mass flow from the primary circuit are calculated in a digital routine with the core and steam generator outlet temperatures as input values.

## 4.3. Boron Acid Distribution

The boron acid concentration in the primary loop is also calculated with a division in compartment, and using the same division as used for the temperature calculations plus four compartments for the core and two extra compartments for the U-tubes in the steam generator. It is assumed that the boron acid is injected into and extracted from the same compartment. This is a useful approximation as the extraction rate is so slow that the concentration may be regarded as uniform in the circuit. The concentration is calculated with an equation similar to (4.11), but with the inclusion of an injection term for the injection compartment:

$$C_b(o, n+1) = (C_b(o, n) + \frac{\Delta t W}{V \rho_f}\ (C_b(i, n+1) + \frac{W_b}{W}))/(1 + \frac{\Delta t W}{V \rho_f}). \qquad (4.14)$$

The concentration distribution is calculated in a digital routine with the boron acid injection rate, $W_b$, as input variable and the boron concentrations in the core compartments as output variables.

Symbols for the primary circuit

| | | |
|---|---|---|
| $A_c$ | : Cross section of the core coolant flow | $m^2$ |
| $De_c$ | : Hydraulic diameter of the cooling channel | m |
| V | : Volume of a compartment in the primary circuit | $m^3$ |
| $V_c$ | : Volume of the coolant in a core section | $m^3$ |
| W | : Flow rate | kg/s |
| $W_c$ | : Flow rate in the core | kg/s |
| $W_b$ | : Flow rate of boron acid to the coolant | kg/s |
| $v_c$ | : Velocity of the coolant in the core | m/s |
| $q_c$ | : Heat flow to the coolant per m core | MW/m |
| $q_t$ | : Part of $q_c$ used for heating of coolant | MW/m |
| $q_b$ | : Part of $q_c$ used for boiling | MW/m |
| $Q_c$ | : Heat flow to the coolant per core section | MW |
| $Q_t$ | : Corresponds to $q_t$ | MW |
| $Q_b$ | : Corresponds to $q_b$ | MW |
| T | : Temperature in the coolant | $^oC$ |
| $T_c$ | : Temperature in the coolant in the core | $^oC$ |
| $T_{ps}$ | : Saturation temperature in the primary circuit | $^oC$ |
| $p_p$ | : Pressure in the primary circuit | bar |
| $\rho_f$ | : Density of water | $kg/m^3$ |
| $\rho_{gs}$ | : Saturation density of steam | $kg/m^3$ |
| $\rho_m$ | : Mean density of coolant in core | $kg/m^3$ |
| $h_{fg}$ | : Evaporation heat of water | MJ/kg |
| $c_p$ | : Specific heat of coolant | $MJ/kg^oC$ |
| $\alpha$ | : Steam volume fraction in core | |
| $C_b$ | : Concentration of boron acid in the coolant | |

Indices:

| | |
|---|---|
| j | : Section number in core |
| n | : Time event. $T = T_o + n \cdot t$ |



| | |
|---|---|
| o | : Outlet for a compartment in the primary circuit |
| i | : Inlet for a compartment in the primary circuit |

## 5. THE PRESSURISER MODEL

The pressuriser dynamics was studied by a two-point non-linear model programmed as an independent digital model. A slightly simplified version was worked out for the station model with due consideration to computing time and the importance of the different effects as studied by the complete model.

Section 5.1 gives a description of the complete independent model and section 5.2 of the simplified version.

### 5.1. A Two-point Non-linear Model

The pressuriser is described by mass and energy balance equations for the water and steam phases regarded as concentrated systems, i.e. as two mass points. Such effects as steam bubble and water drop transit times and non-uniform temperature distribution are consequently neglected. Heat transfer between the two phases is neglected as well, whereas heat transfer between the steam phase and the tank wall is included, but only in a simple way as it is shown to be non-important.

Both the water and the steam phase may exist in two conditions: saturated and non-saturated, i.e. superheated steam or subcooled water. Different equations must be used for the two conditions, and proper switching conditions must be included in the model.

The equations are given in a reduced form ready for programming. They are easily derived from the basic mass and energy balance equations using Appendix A.

The equations for the water phase in saturation are:

$$\dot{V}_f = \frac{1}{\rho_{fs}} \left(W_i + W_c - W_e - V_f \frac{d\rho_{fs}}{d p_s} \dot{p}\right), \qquad (5.1a)$$

$$W_e = \frac{1}{h_{fg}} \left(Q - W_i^+ (h_{fs} - h_i) - V_f \left(\rho_{gs} \frac{d h_{fs}}{d p_s} - 0.1\right) \dot{p}\right). \qquad (5.2a)$$

For the subcooled condition, the corresponding equations are:

$$\dot{V}_f = \frac{1}{\rho_f} \left(W_i + W_c - V_f \left(\left(\frac{\partial \rho_f}{\partial h}\right)_p \dot{h}_f + \left(\frac{\partial \rho_f}{\partial p}\right)_h \dot{p}\right)\right) \qquad (5.1b)$$

$$\dot{h}_f = \frac{1}{V_f \rho_f} (Q + W_c(h_{fs} - h_f) - W_i^{+}(h_f - h_i) + 0.1\, V_f \dot{p}) . \qquad (5.2b)$$

The switching from saturation to subcooling takes place when $W_e$ reaches zero from the positive direction. $W_e$ remains zero in the subcooled state. The water phase returns to the saturation state when $h_f$ reaches $h_{fs}$ from the lower side. In the saturation state $h_f$ is identical to $h_{fs}$.

The equations for the steam phase in saturation are:

$$\dot{p} = \frac{1}{V_g \frac{d\rho_{gs}}{d p_s}} (\rho_{gs} \dot{V}_f + W_e + W_k - W_c - W_r) , \qquad (5.3a)$$

$$W_c = \frac{1}{h_{fg}} (W_k(h_{gs} - h_k) + V_g(\rho_{gs} \frac{d h_{gs}}{d p_s} - 0.1)\, \dot{p} + Q_{gv}). \qquad (5.4a)$$

For the superheated condition the corresponding equations are:

$$\dot{p} = \frac{1}{V_g (\frac{\partial \rho_g}{\partial p})_h} (W_e + W_k - W_r + \rho_g \dot{V}_f - V_g (\frac{\partial \rho_g}{\partial h})_p \dot{h}_g), \qquad (5.3b)$$

$$\dot{h}_g = \frac{1}{V_g \rho_g} (W_e(h_{gs} - h_g) - W_k(h_g - h_k) + 0.1\, V_g \dot{p} - Q_{gv}). \qquad (5.4b)$$

The switching from saturation to superheating takes place when $W_c$ reaches zero from the positive direction. $W_c$ remains zero in the superheated state. The steam phase returns to the saturation state when $h_g$ reaches $h_{gs}$ from the higher side. In the saturation state $h_g$ is identical to $h_{gs}$.

The heat transfer term, $Q_{gv}$, between the steam phase and the tank wall is calculated with a constant heat transfer coefficient and constant heating surface. Further, the heat resistance in the wall and the heat losses from the wall outside are neglected; this means that the exchange is assumed to take place between the steam phase and a thermal capacity connected by a constant heat resistance. The equations are:



$$\Delta T_g = \frac{d T_s}{d p_s}(p - p_o) + \frac{1}{c_{pg}} (h_g - h_{gs}) , \qquad (5.5)$$

$$Q_{gv} = k_{qgv}(\Delta T_g - \Delta T_v), \qquad (5.6)$$

$$\dot{T}_v = \frac{Q_{gv}}{C_v} . \qquad (5.7)$$

For a real pressuriser, the thermal heating Q, the spray cooling $W_k$ and the steam discharge $W_r$ are discontinuous functions of the pressure deviation $(p - p_o)$. For simplicity, continuous control functions with deadband are used in the model; this just means that the variables change more smoothly. The equations are:

$$Q = A_q(p - p_o + \Delta p_g)^{-} , \qquad (5.8)$$

$$W_k = A_k(p - p_o - \Delta p_k)^{+} , \qquad (5.9)$$

$$W_r = 0 \qquad \text{for } p - p_o < \Delta p_r, \qquad (5.10)$$

$$W_r = \text{const.} \qquad \text{for } p - p_o \geq \Delta p_r.$$

The sign at the upper right corner of an expression means that the expression is only used when it is positive or negative respectively; otherwise it is equal to zero.

The parameters for steam and water are approximated by polynomials of first to third order. For the non-saturation states the parameters are actually functions of two variables, but for the near saturation state an approximation by functions of only one variable is of sufficient accuracy.

In the steady state a small spray cooling is used together with some heating power in the water phase to keep both phases in the saturation condition giving the best absorbtion of volume expansion in the primary loop. The time derivatives in the steady state are zero, which gives a set of initial conditions for transient calculations:

$$W_{ko} = \frac{Q_o}{h_{gs} - h_k - h_{fg}}$$

$$W_i = - W_k \qquad (5.11)$$

$$W_e = \frac{Q}{h_{fg}}$$

$$W_c = W_e + W_k ,$$

where the selection of Q determines the initial values.

## 5.2. A Simplified Pressuriser Model

The model described in section 5.1 was used to calculate transients for an impulse input function for $W_i$ of both square and triangular wave form. Transients in all variables were studied for the influence of different effects. It appears that the transition between saturation and non-saturation for the water phase is very important, as expected, while the transition between the corresponding states for the steam is of minor importance. Also heat transmission to the tank wall is without significance until the heat transfer coefficient reaches the order of 25 kw/$^{o}$C m$^2$, a value which is larger than normal values. For a square impulse input function of $W_i$ the transition to steam superheating is most influential, but even in this case the influence on the pressure peak is less than 5%. For a more smooth impulse form, as produced by the reactor circuit, the influence is smaller.

The simplified model is described by the equations in section 5.1 except (5.3b), (5.4b) and (5.5)to (5.7) with the term $Q_{gv}$ equal to zero in equation (5.4a). The steam saturation condition is "frozen", even when $W_c$ goes slightly negative. Further, a time lag function is inserted for the inlet flow due to noise originating from the hybrid computations for the core; the time lag is chosen at 0.5 sec at present.

Fig. 7 gives a comparison of transients for the two models. The simplified model gives somewhat higher pressure deviations especially in the time interval 10 - 80 sec, but the agreement is found to be satisfactory.

The flow rate $W_i$ is equal to the net mass flow rate from the primary circuit as calculated in section 4.2. The corresponding enthalpy $k_i$ results from the mixing process in the surge tube. It is divided into three compart-



ments assuming ideal mixing in each of them. The equations correspond to eq. (4.11):

$$h(j+1, n+1) = (h(j+1, n) + \frac{\Delta t\, W_i}{V\, \rho_f}\, h(j, n+1))/(1 + \frac{\Delta t\, W_i}{V\, \rho_f}). \qquad (5.12)$$

For $W_i > 0$ the calculation is carried out upwards from the hot leg in the primary circuit; for $W_i < 0$ the calculation goes in the direction opposite to the pressuriser.

Both models are implemented by digital programs using simple Euler integration. This is sufficient for the model included in the total station model, as the input function, the surge flow $W_i$, only varies relatively slowly as a smooth, continuous time function. For the independent model, however, where impulse input must be allowed, an iterative calculation of the algebraic variables is necessary between the integration steps due to the strong interaction between the equations and the phase shifts for the water and steam phase. Otherwise false damped oscillations in $\dot{p}$ would be induced by an stepwise change in $\dot{p}$, originating from either a step in $W_i$ or a phase shift for the steam phase.

### Symbols for the pressuriser model

| | | |
|---|---|---|
| $V_f$ | : Volume of the water phase | $m^3$ |
| $V_g$ | : Volume of the steam phase | $m^3$ |
| $W_i$ | : Inlet mass flow rate from surge tube | kg/s |
| $W_i^+$ | : $W_i$ limited to positive values | |
| $W_k$ | : Coolant inlet mass flow rate | kg/s |
| $W_c$ | : Condensation mass flow rate from steam to water phase | kg/s |
| $W_e$ | : Evaporation mass flow rate from water to steam phase | kg/s |
| $W_r$ | : Mass flow rate through the pressure relief valve | kg/s |
| Q | : Heating power | MW |
| $Q_{gv}$ | : Heat flow between steam phase and steel wall | MW |
| $\rho$ | : Density | |
| h | : Enthalpy | |
| p | : Pressure | |

$c_{pg}$ : Specific heat capacity for steam — MJ/kg $^{o}$C

$C_v$ : Heat capacity for the steel wall — MJ/$^{o}$C

$k_{qgv}$ : Heat transfer coefficient between steam and wall — MW/$^{o}$C

Indices

f : water phase

g : steam phase

s : saturation state

k : coolant inlet condition

i : surge flow inlet condition

v : steel wall

## 6. THE STEAM GENERATOR MODEL

Next to the reactor, the steam generator is the most important unit for power plant dynamics, so it was studied in some detail by an independent program. The results of the investigations were used to check the validity of a simplified version for the complete station model.

There are various types of steam generators; we have chosen a Westinghouse type with U-tube without preheater at the feedwater entrance. A simplified diagram of the physical structure is shown in fig. 8.

For simulation purposes the steam generator is divided into eight sections, as shown by dashed lines in fig. 8. For both models the seven sections outside the core are described by normal differential equations; but the description of the core is far more detailed for the independent than for the simplified model.

The detailed model is described in 6.1 and the simplified model in 6.2.

### 6.1. The Detailed, One-dimensional Model

Main emphasis has been placed upon a detailed description of the dynamic properties of the heat transfer and the water-steam flow in the core. For this reason the core is divided into a number of sections along the vertical axis, in the present version 20 sections, giving 40 sections along the U-tubes.

Some fundamental approximations are used for the formulation of the equations. These are:



a. Use of uniform water and steam velocity on the primary and the secondary side and constant steam to water velocity ratio (slip factor).

b. No subcooled boiling is included. The water is heated to saturation and afterwards all the energy is used for steam production.

c. Thermal equilibrium at the saturation point is assumed in the boiling part of the core, the riser, the steam volume and the upper part of the feedwater chamber.

d. No heat conduction takes place along the tubes. The tubes are divided into two shells each with half of the heat capacity and with all the heat resistance between the shells.

e. No boiling is allowed in the downcomer and no heat transmission takes place from the core. This assumption limits the working range of the pressure time derivative to values less than 1-2 bar/s dependent on the power level.

f. All heat exchange with the wall and the steel constructions in the steam volume is neglected.

The basic equations are given in sections 6.1.A to 6.1.F. Section 6.1.G contains a discussion of the problems arising from the digital simulation and a rearrangement of some of the equations.

#### 6.1.A. The Core

The temperature in the primary circuit and the non-boiling part of the secondary circuit is described by the two partial differential equations:

$$\frac{\partial T_p}{\partial z} = -\frac{1}{W_p}\left(\frac{q_p}{c_{pp}} + A_p \rho_f \dot{T}_p\right) \qquad (6.1.1)$$

$$\frac{\partial T_s}{\partial x} = \frac{1}{W_s}\left(\frac{q_s}{c_{ps}} - A_s \rho_{fs} \dot{T}_s\right) \qquad (6.1.4a)$$

The z-axis travels up and down along the U-tubes and the x-axis travels from the bottom to the top of the core. The U-tubes are substituted by two straight tubes, with an artificial connection at the top. This means that the core can be treated as a parallel flow and a counter flow heat exchanger with common secondary flow and with the primary output from the first as the primary input to the second.

The heat capacity $c_p$ and the density $\rho_f$ are taken as functions of temperature assuming constant pressure, as the pressure influence is small at a certain distance from the saturation point. However, at the secondary side, where the temperature is the saturation temperature, $c_{ps}$ is calculated from the curve for 50 bar extended by "near saturation values" up to 300°C.

The two tube shell temperatures are described by ordinary differential equations for sections of unit length with constant temperature within a section.

$$\dot{T}_{r1} = \frac{2}{C_r} (q_p - q_r) , \qquad (6.1.2)$$

$$\dot{T}_{r2} = \frac{2}{C_r} (q_r - q_s) . \qquad (6.1.3)$$

In the boiling part of the secondary side equation (6.1.4a) is substituted by two equations (6.1.4b) and (6.1.4c) giving the steam and water flow:

$$\frac{\partial}{\partial x} (v_g \alpha) = \frac{1}{h_{fg} \rho_{gs}} \left( \frac{q_s}{A_s} - \dot{p} \left( \alpha \left( \rho_{gs} \frac{d h_{gs}}{d p_s} + h_{fg} \frac{d \rho_{gs}}{d p_s} \right) \right. \right.$$

$$\left. \left. + (1-\alpha) \rho_{fs} \frac{d h_{fs}}{d p_s} - 1 \right) \right) - \dot{\alpha} . \qquad (6.1.4b)$$

$$\frac{\partial}{\partial x}(v_f(1-\alpha)) = \dot{\alpha}(1 - \frac{\rho_{gs}}{\rho_{fs}}) - \dot{p}(\frac{\alpha}{\rho_{fs}} \frac{d\rho_{gs}}{d p_s} + \frac{1-\alpha}{\rho_{fs}} \frac{d \rho_{fs}}{d p_s}) - \frac{\rho_{gs}}{\rho_{fs}} \frac{\partial}{\partial x}(v_g \alpha) \qquad (6.1.4c)$$

The equations (6.1.4b) and (6.1.4c) are derived from the basic continuity mass and energy balance equations. The derivation may be found in Appendix B.

The heat transfer is calculated according to the Dittus-Boelter equation or, in the boiling region, according to the Thom equation.

The Dittus-Boelter equation is:

$$\frac{h\, De}{\lambda} = 0.023 \left(\frac{De\, G}{\eta}\right)^{0.8} \left(\frac{c_p \eta}{\lambda}\right)^{n}$$

where $n = 0.4$ for cooling and 0.3 for heating. G is the mass flow rate per unit area.



The heat transfer coefficient h can be written as:

$$h = 0.023 \frac{G^{0.8}}{De^{0.2}} H(p, T),$$

where

$$H(p, T) = \frac{c_p^{\,n} \lambda^{1-n}}{\eta^{0.8-n}} .$$

The function H(p, T) is shown in figs. 9 and 10 for $n = 0.4$ and 0.3 respectively, corresponding to the primary and secondary side. The influence of the pressure is small except near saturation at 150 bar, and this area is not used. With a reasonably good accuracy the functions may be represented by straight lines or better by higher order polynomials independent of pressure.

The Thom equation gives the heat transfer in the following form:

$$q = 1.972 \exp\left(\frac{p}{43.4}\right) (T_{r2} - T_{sa})^2 .$$

Due to the boiling heat transfer mechanism the heat flow is proportional to the square of the difference between the metal surface and saturation temperature. This equation is used when it gives a higher heat flow than the Dittus-Boelter equation.

The heat transmission equation for the primary side giving the heat flow per unit length of the tubes will then be:

$$q_p = \frac{0.023\ E\text{-}3}{De_p^{0.2}} O_p \left(\frac{W_p}{A_p}\right)^{0.8} H_p(T) (T_p - T_{r1}) ; \qquad (6.1.5)$$

and for the secondary side one of the two equations:

$$q_s = \frac{0.023\ E\text{-}3}{De_s^{0.2}} O_s \left(\frac{W_s}{A_s}\right)^{0.8} H_s(T) (T_{r2} - T_s), \quad \text{or} \qquad (6.1.7a)$$

$$q_s = (1.972\ E\text{-}3) \exp\left(\frac{p}{43.4}\right) (T_{r2} - T_{sa})^2 . \qquad (6.1.7b)$$

The equation, (6.1.7a) or (6.1.7b), that gives the highest value of q is selected. The total $q_s$ in equation (6.1.4) is the sum of two terms from the tube sections at the same height in the upstream and downstream leg of the U-tube. The units for q in eqs. (6.1.5) and (6.1.7) are MW/m when

MKS units are used for the other variables and H has the dimension given in figs. 9 and 10.

The heat flow per unit length through the tube wall is given by:

$$q_r = \frac{\lambda_r}{\Delta r} O_r (T_{r1} - T_{r2}) . \qquad (6.1.6)$$

In the boiling region eqs. (6.1.4b) and (6.1.4c) are used to calculate the volume flows ($v_g a$) and ($v_f(1-a)$) along the tubes. When these flows are known the void fraction a may be calculated as:

$$a = \frac{(v_g a)/S}{(v_g a)/S + (v_f(1-a))} , \qquad (6.1.8)$$

using the relation $v_g = S\, v_f$ where the slip factor S is taken as a constant.

The steam quality X is calculated as:

$$X = \frac{(v_g a)\ \rho_{gs}}{(v_g a)\ \rho_{gs} + (v_f(1-a))\ \rho_{fs}} . \qquad (6.1.9)$$

The steam quality is used to calculate the friction pressure drop in the boiling region. The two-phase friction is calculated according to Becker as the one-phase friction multiplied by the two-phase friction multiplier R. The pressure drop across $\Delta x$ is then:

$$\Delta p = f \frac{\Delta x}{2 De} \rho\ v^2 R ,$$

where the friction coefficient f is:

$$f = 0.184\ R_e^{-0.2} \qquad R_e = \frac{1}{\eta} De\, v \rho ,$$

and the two phase friction multiplier R is taken as:

$$R = 1 + 2400 \frac{X}{p} .$$

Introducing f, $R_e$ and R in the equation for $\delta p$ we obtain:

$$\Delta p = 0.092 \frac{\Delta x}{De^{1.2}}\ v^{1.8}\ \rho^{0.8}\ \eta^{0.2} (1 + 2400 \frac{X}{p}).$$

The calculation can be simplified by expressing the pressure drop



relative to the density and introducing the function $F_f(T)$

$$F_f(T) = (\frac{\eta}{\rho})^{0.2} .$$

The pressure drop across one section of the core then takes the form:

$$\frac{\Delta p_1}{\rho_{fs}} = 0.092 \frac{\Delta x}{De_s^{1.2}}\ v^{1.8}\ F_f(T)\ (1 + 2400 \frac{X}{p}). \qquad (6.1.10)$$

$F_f$ is the only factor dependent of temperature. It is shown in fig. 11 and appears to be independent of pressure; furthermore it is fairly constant in a large temperature range. For simplification we use $F_f(T) = 0.0425$ $(\frac{m^2}{s})^{0.2}$. The velocity v should be the total mass flow divided by the flow area and the density,

$$v = \frac{W_g + W_f}{A_s\ \rho_{fs}} = v_f(1-a) + (v_g a) \frac{\rho_{gs}}{\rho_{fs}} . \qquad (6.1.10a)$$

## 6.1.B. The Hydraulic Loop

The secondary circulation rate is governed by the void volume and the friction forces, which in the steady state neutralize each other. Besides the pressure drop in the core we have pressure drops in the downcomer, the riser, the feedwater chamber and at the inlet to the core. Only the first of these can be calculated, the others can only be estimated. Thus they are included in the total pressure drop by a multiplication factor in connection with the downcomer, assuming that all of them depend on the water velocity in the same way.

Using the same procedure as for the core the downcomer pressure drop becomes:

$$\frac{\Delta p_2}{\rho_{fs}} = 0.092 \frac{L'_d}{De_d^{1.2}} F_f(T)\ v_d^{1.8} . \qquad (6.1.11)$$

The effective length of the downcomer is equal to $L_d$ multiplied by the correction factor mentioned above. For lack of better knowledge $L'_d$ is used as $2\ L_d$.

The momentum equation is derived as shown in Appendix B and used to calculate the circulation velocity. We use equation B9 from the appendix with the term L equal to zero.

$$\frac{dJ}{dt} = D - \Delta p_f .$$

The momentum J is the momentum per unit area for the closed loop. The driving force D and the friction pressure drop $\Delta p_f$ are:

$$D = g(\rho_{fs} - \rho_{gs}) \sum_{\Delta x} \alpha \Delta x ,$$

$$\Delta p_f = \Delta p_2 + \sum_{\Delta x} \Delta p_1 .$$

In the first term of the expression for D, $\rho_{gs}$ is small compared with $\rho_{fs}$ and will be neglected in the following.

The momentum J must be calculated for both single-phase and two-phase flow sections.

For the two-phase flow the momentum will be calculated assuming that the total mass flow takes place in the water phase. This means that we neglect the extra momentum originating from the slip ratio. The water velocity at a given position is multiplied by the factor $1/(1-\alpha)$, while the density is multiplied by $(1-\alpha)$ so the product $\rho v$ remains constant along the channel.

For all sections the velocity will be referred to the downcomer by the relation $v_y A_y = v_d A_d$.

Introducing these simplifications and dividing by $\rho_{fs}$ leads to the final form of the equation:

$$\sum_y L_y \frac{A_d}{A_y} \dot{v}_d = g \sum_{\Delta x} \alpha \Delta x - \frac{\Delta p_2}{\rho_{fs}} - \sum_{\Delta x} \frac{\Delta p_1}{\rho_{fs}} . \qquad (6.1.12)$$

On the left side the summation is carried out for all sections in the closed loop, while the summation on the right side is over the core only. The sum on the left side is dominated by the downcomer; this reduces the influence of the simplifications.

The secondary mass flow is finally calculated from $v_d$ as:

$$W_s = A_d \, v_d \, \rho_{fs} . \qquad (6.1.13)$$

The saturation value of the density is used here as in equation (6.1.12) since the temperature will always be quite near the saturation point.



## 6.1.C. The Riser and the Steam Volume

Due to the complicated mechanism of the steam-water separators in the riser, a detailed description of the steam-water distribution is impossible, so only a rough approximation is used. It is assumed that the void fraction is equal to the output value for the core throughout the riser in the steady state and follows dynamically with a time lag equal to the transit time for a steam particle:

$$\dot{\alpha}_r = \frac{1}{\tau_r} (\alpha_o - \alpha_r) \qquad (6.1.14)$$

$$\tau_r = \frac{V_r}{A_s \, v_{go}} = \frac{V_r \, \rho_{gs} \, \alpha_o}{W_{go}} . \qquad (6.1.15)$$

It is further assumed that the water and steam phase is in thermal equilibrium at the system pressure during transients. In this respect the water in the upper part of the feed water chamber is included in the water volume of the riser. Thermal equilibrium means that mass transfer between the two phases takes place.

The energy equation for the steam volume and the riser leads to the following equation:

$$(V_e + \alpha_r V_r) \frac{d\rho_{gs}}{dp_s} \dot{p} = W_{go} - W_l - V_r \dot{\alpha}_r \rho_{gs} - C1 \, \dot{p}$$

$$C1 = \frac{1}{h_{fg}} \left(\rho_{fs} \frac{dh_{fs}}{dp_s} (V_{bh} + V_r(1-\alpha_r)) + (V_e + \alpha_r V_r) \rho_{gs} \frac{dh_{gs}}{dp_s} - (V_{bh} + V_r + V_e)\right).$$

The term $C1 \cdot \dot{p}$ represents the mass exchange with the water during pressure variations. C1 may be somewhat simplified: $(V_e + \alpha_r V_r)$ can be used as a constant volume because the variable term $\alpha_r V_r$ will always be small compared with $V_e$; and $(V_{bh} + V_r + V_e)$ can be reduced to the same volume as that used for $(V_e + \alpha_r V_r)$ because $(\rho_{fs} \frac{dh_{fs}}{dp}) \gg 1$ (note that $\rho \frac{dh}{dp}$ has the dimension 1). So $\dot{p}$ may be written as:

$$\dot{p} = (W_{go} - W_l - V_r \dot{\alpha}_r \rho_{gs}) / ((V_e + \alpha_{rm} V_r) \frac{d\rho_{gs}}{dp_s} + C1) \qquad (6.1.16)$$

$$C1 = \frac{1}{h_{fg}} \left(\rho_{fs} \frac{dh_{fs}}{dp_s} (V_{bh} + V_r(1-\alpha_r)) + (V_e + \alpha_{rm} V_r)\left(\rho_{gs} \frac{dh_{gs}}{dp_s} - 1\right)\right).$$

The steam load $W_l$ is taken as a load constant $C_i$ multiplied by the pressure:

$$W_l = C_l\, p\,. \tag{6.1.17}$$

The steam load is varied by variation of $C_l$.
The water flow to the feed water chamber will be:

$$W_b = W_{fo} + C1\, \dot{p} + V_r\, \dot{a}_r\, \rho_{fs}\,. \tag{6.1.18}$$

## 6.1.D. The Feedwater Chamber

The energy equation for the lower part of the feedwater chamber is used to calculate the temperature assuming complete mixture of the feed water with the recirculating water:

$$\dot{h}_b\, V_{bl}\, \rho_f = W_b\,(h_{fs} - h_b) + W_i\,(h_i - h_b).$$

Introducing the heat capacity $c_{ps}$ for the recirculating water at saturation, $c_{pm} = \frac{1}{2}(c_{pi} + c_{ps})$ for the feedwater, and as an approximation using $c_{ps}$ for the mixture, gives us:

$$T_b = \frac{1}{V_{bl}\rho_{fs}}\,(W_b(T_{sa} - T_b) + W_i\,\frac{c_{pm}}{c_{ps}}(T_i - T_b)). \tag{6.1.19}$$

The ratio $\frac{c_{pm}}{c_{ps}}$ can be taken as a constant value equal to 0.94 with an error less than 3% in the pressure range 50-75 bar and a feedwater temperature of 210-240°C.

The water level changes may be calculated as:

$$\Delta L_f = \frac{1}{A_b\,\rho_{fs}}\,(W_b + W_i - \dot{p}\,\frac{d\rho_{fs}}{dp_s}\,\Sigma V)\,, \tag{6.1.20}$$

where V is the sum of all water volumes outside the core. It is assumed that the overall temperature dynamically follows the saturation temperature.

## 6.1.E. The Downcomer

The downcomer is separated from the core by a steel shield. As the temperature difference across the shield is less than 5°C, and the heating surface less than 5% of the U-tube surface, the heat transmission through the shield can be neglected. It is further assumed that the pressure



variations are so slow that boiling is avoided in the downcomer. This means that $\dot{p} < \frac{dp}{dT}\,\frac{\Delta T}{\Delta t}$, where $\Delta T \simeq 4^oC$, $\Delta t \simeq 2$ s and $\frac{dp}{dT} \simeq 1$ bar/°C.

The energy equation then gives:

$$\frac{\partial T_d}{\partial x} = -\,\frac{1}{W_s}\,A_d\,\rho_{fs}\,\dot{T}_d\,, \tag{6.1.21}$$

with the direction of the x-axis from the top to the bottom.

## 6.1.F. The Inlet and Outlet Chambers

The inlet and outlet chambers in the primary loop are not important since they are small and without heat exchanges with the surroundings. Each introduces a time lag of approximately 1 sec at normal primary flow rate. The two equations are:

$$\dot{T}_{p1} = \frac{W_p}{V_{pi}\,\rho_f}\,(T_{pi} - T_{p1})\,, \tag{6.1.22}$$

$$\dot{T}_{p2} = \frac{W_p}{V_{po}\,\rho_f}\,(T_{po} - T_{p2})\,. \tag{6.1.23}$$

## 6.1.G. Solution by a Digital Program

The differential equations are solved by division of the space axis into subsections and by sampling in the time domain using first-order differences for the derivatives. This gives the most simple program, but a careful procedure has to be used when solving the equations to obtain a stable solution with reasonable dynamic accuracy.

The most stable and accurate solution is obtained by calculation of the space derivative for the next step in space and time, as function of the variables taken as mean values of both the space and time step concerned. However, the time derivative, for reasons of stability, must always be evaluated at the end of the space section. This procedure demands feedback in the equations and parallel solution of several equations, which by pure digital programming leads to iterations or the solution of a large set of coupled equations.

Another important problem is the simultaneous integration along the primary and secondary space axis, which by digital methods can only be accomplished through time-consuming iterations.

The present chapter describes how the basic equations are used and how the problems mentioned above are solved.

Eqs. (6.1.1) and (6.1.4) have extremely strong feedback from $\dot{T}$ and $\dot{\alpha}$ which it is absolutely necessary to take into account in the solution. This is done quite simply in the temperature equations. We introduce the following approximations:

$$\dot{T}(j+1,\ n+\tfrac{1}{2}) = \frac{1}{\Delta t}(T(j+1,n+1) - T(j+1,n)),$$

$$\frac{\partial}{\partial x}(T(j+\tfrac{1}{2},\ n+1)) = \frac{1}{\Delta x}(T(j+1,\ n+1) - T(j,n+1)).$$

The integers j and n stand for the space and the time step respectively. Introduction into eq. (6.1.1) and solving with respect to $T_p(j+1,n+1)$ gives:

$$T(j+1,n+1)=(-\frac{q_p}{W_p c_{pp}} + \frac{A_p\rho_f}{W_p\Delta t}T_p(j+1,n) + \frac{1}{\Delta z}T_p(j,n+1))/(\frac{1}{\Delta z}+\frac{A_p\rho_f}{W_p\Delta t}).$$

Eq. (6.1.4a) is changed similarly:

$$T_s(j+1,n+1)=(\frac{q_s}{W_s c_{ps}} + \frac{A_s\rho_{fs}}{W_s\Delta t}T_s(j+1,n)+\frac{1}{\Delta x}T_s(j,n+1))/(\frac{1}{\Delta x}+\frac{A_s\rho_{fs}}{W_s\Delta t}).$$

Eqs. (6.1.4b) and (6.1.4c) are more complicated as $\dot{\alpha}$ cannot be introduced as a simple function of one of the two variables $(v_g\alpha)$ or $(v_g(1-\alpha))$. We use eqs. (6.1.4b), (6.1.4c) and (6.1.8) to find an explicit solution to $\alpha(j+1,\ n+1)$.

For convenience we introduce the following short notations:

$$C2 = h_{fg}\,\rho_{gs}$$

$$C3 = \rho_{gs}\frac{dh_{gs}}{dp_s} + h_{fg}\frac{d\rho_{gs}}{dp_s}$$

$$C4 = \rho_{fs}\frac{dh_{fs}}{dp_s}$$

$$C6 = \frac{1}{\rho_{fs}}\frac{d\rho_{gs}}{dp_s}$$

$$C7 = \frac{1}{\rho_{fs}}\frac{d\rho_{fs}}{dp_s}$$



$$C8 = \frac{\rho_{gs}}{\rho_{fs}}$$

$$\alpha' = \tfrac{1}{2}(\alpha(j,n+1) + \alpha(j+1,n))$$

$$\alpha_g = \alpha(j+1,n)$$

$$\alpha = \alpha(j+1,n+1)$$

$$QS1 = (\frac{q_s}{A_s} - \dot{p}(\alpha' C3 + (1-\alpha')C4 - 0.1))/C2$$

$$QS2 = -\dot{p}(\alpha' C6 + (1-\alpha')C7)$$

$$UG = v_g\alpha(j,n+1)$$

$$UF = v_f(1-\alpha)(j,n+1).$$

From eqs. (6.1.4b) and (6.1.4c) we find:

$$\Delta UG = \Delta x\frac{\partial}{\partial x}(v_g\alpha) = \Delta x\,QS1 - \frac{\Delta x}{\Delta t}(\alpha-\alpha_g)$$

$$\Delta UF = x\frac{\partial}{\partial x}(v_f(1-\alpha)) = (1-C8)\frac{\Delta x}{\Delta t}(\alpha-\alpha_g) + \Delta x\ Qs2 - C8\ \Delta UG.$$

Insertion in eq. (6.1.8) gives:

$$\alpha\,(UG + \Delta x\,QS1 - \frac{\Delta x}{\Delta t}(\alpha-\alpha_g))$$

$$+ \alpha\cdot S\,(UF + (1-C8)\frac{\Delta x}{\Delta t}(\alpha-\alpha_g) + \Delta x\,QS2 - C8\,\Delta x\,QS1 + C8\frac{\Delta x}{\Delta t}(\alpha-\alpha_g))$$

$$= UG + \Delta x\,QS1 - \frac{\Delta x}{\Delta t}(\alpha-\alpha_g),$$

which after reduction takes the form:

$$A\alpha^2 + B\alpha + C = 0,$$

where

$$A = \frac{\Delta x}{\Delta t}(S-1)$$

$$B = UG + S\,UF + \Delta x\,(QS1 + S(QS2 - C8\,QS1) - \frac{1}{\Delta t}(\alpha_g(S-1)-1))$$

$$C = -(UG + \Delta x\,(QS1 + \frac{1}{\Delta t}\alpha_g)).$$

NB: The unit for power used here is MW, therefore the constant 1 in QSI has been changed to 0.1.

The solution gives:

$$\alpha = (-B + (B^2 - 4AC)^{0.5})/2A.$$

The shift from temperature calculation to void calculation takes place when a value of $T_s(j+1, n+1)$ exceeds the saturation value. For this section the output value of $T_s$ is fixed to $T_{sa}$ and the length of the boiling part of the section $\Delta x'$ is calculated as:

$$\Delta x' = \Delta x \frac{T_s(j+1, n+1) - T_{sa}}{T_s(j+1, n+1) - T_s(j, n+1)},$$

and used in the calculation of $\alpha$ from the formulae given above.

In the calculation of the temperature and void profiles for the time step $n+1$ by integration of (6.1.1) - (6.1.4) we should use heat flows taken at time $n + \frac{1}{2}$:

$$q(n + \tfrac{1}{2}) = \tfrac{1}{2}(q(n) + q(n+1)),$$

but generally this is impossible. Therefore we perform the calculations for q taken at time n and store the results as temporary profiles. The calculations are then repeated with the heat flow calculated on the basis of these temporary profiles, and finally we use a mean value of the two results. This procedure corresponds to the improved Euler integration method. However, in the primary and the secondary temperature calculations, where it is possible to improve the stability and accuracy by using the mean temperature

$$T_m = \tfrac{1}{2}(T(j, n+1) + T(j+1, n))$$

for the heat flow calculation, this mean temperature is used.

Together with the void calculations for the subsections of the core we calculate the friction pressure drop also as a mean value between two steps. Afterwards we calculate the driving force from the void distribution at time $n+1$, the pressure drop outside the core from the velocity $v_d$ at time n, and finally, by simple Euler integration, the velocity $v_d(n+1)$.

The pressure is calculated in a straight forward manner from eq. (6.1.16) by Euler integration, but the internal feedback from mass exchange



between steam and water has been taken into account. Only the small feedback term $\Delta W_o = \Delta p \cdot \Delta C_1$ is neglected as it appears to affect the accuracy much less than the uncertainty in the steam volume. However, step changes in $C_1$ may start damped oscillations in $\dot{p}$ due to the missing feedback. These oscillations may be avoided using a time lag, equal to the sampling time, for $\dot{p}$.

## 6.2. The Simplified Steam Generator Model

The simplification mainly consists of two points:

a. The subsections in the core and the downcomer are separately lumped together in one section.

b. Some slightly varying parameters are substituted by constant values.

The lumped core model gives no information on the void distribution, so an empirical relation between the void volume and the outlet void fraction is introduced, and the two-phase friction drop is calculated in a similar way.

The present chapter gives all the equations for the sake of completeness, even though some of them are identical with the corresponding ones in chapter 6.1.

The equations for the primary inlet and outlet chambers are transferred to the primary loop described in section 4.

The core primary outlet temperature is the most delicate one to describe by one space node. It may be written as a sum of two terms:

$$T_{po} = T_{pl,n} - \Delta T_{po}, \qquad (6.2.1)$$

where $T_{pl,n}$ is the inlet temperature $T_{pl}$ delayed $\tau_p = V_p \rho_f / W_p$, and $\Delta T_{po}$ is the temperature drop resulting from the heat transfer. $\Delta T_{po}$ may be calculated by a single time lag equal to the transit time for a water particle:

$$\dot{\Delta T}_{po} = \frac{1}{V_p \rho_f}\left(\frac{Q_p}{c_{pp}} - W_p \Delta T_{po}\right). \qquad (6.2.1a)$$

In the same way $T_{pl,n}$ could be calculated with the same time lag. However, this would be the poorest approximation to a time delay. On the other hand, division into many sections and calculation of $T_{pl,n}$ by a series of time lags would require too much calculation equipment or time, and, as shown by experiments, give a poor transient response in connection

with the approximation in eq. (6.2.1a). The optimal number of sections has appeared to be two. The equations for $T_{pl,n}$ will then be:

$$\dot{T}_{pl,1} = \frac{2\,W_p}{V_p\,\rho_f}\,(T_{pl} - T_{pl,1})\,. \qquad (6.2.1b)$$

$$\dot{T}_{pl,2} = \frac{2\,W_p}{V_p\,\rho_f}\,(T_{pl,1} - T_{pl,2}). \qquad (6.2.1c)$$

The mean value of the primary temperature $T_p$ is calculated as a weighted sum of inlet and outlet temperature and used for the heat transfer calculation,

$$T_p = a_p\,T_{pl} + (1 - a_p)\,T_{po}\,. \qquad (6.2.2)$$

The weighting factor $a_p$ is chosen tc give the best possible mean value of $T_p$ along the U-tubes for the working range 25-100% of full load. The temperature distribution $T_p(x)$ is calculated by the detailed model.

As in section 6.1, the wall of the U-tubes is divided into two shells each described by first-order equations:

$$\dot{T}_{r1} = \frac{2}{C_r\,L_c}(Q_p - Q_r), \qquad (6.2.3)$$

$$\dot{T}_{r2} = \frac{2}{C_r\,L_c}(Q_r - Q_s). \qquad (6.2.4)$$

The heat flows $Q_p$, $Q_r$ and $Q_s$ are calculated as follows:

$$Q_p = \frac{0.023\ E\text{-}3}{De_p^{0.2}}\,Q_p\,L_c\,(\frac{W_p}{A_p})^{0.8}\,H_p\,(T_p - T_{r1}), \qquad (6.2.5)$$

$$Q_r = \frac{O_r\,L_c}{\Delta r}\,\lambda_r\,(T_{r1} - T_{r2}), \qquad (6.2.6)$$

$$Q_s = (1.972\ E\text{-}3)\,O_s\,L_c\,\exp(\frac{p}{43.4})\,(T_{r2} - T_{sa})^2\,. \qquad (6.2.7)$$

Calculation of $Q_s$ is based only on eq. (6.1.7b) which is the dominating one of the two forms a and b. Equation (6.1.7a) will normally only be used for less than 10% of the heat transport.

The heat flow to the secondary side $Q_s$ is divided into two terms: $(Q_s - Q_k)$ used to heat the water from the inlet temperature $T_d$ to the saturation temperature $T_{sa}$, and $Q_k$ available for steam production.



$$Q_k = Q_s - W_s\,c_{ps}\,(T_{sa} - T_d). \qquad (6.2.8)$$

On the secondary side the energy and mass balance equations give the total void volume and the water outlet flow:

$$\dot{V}_g = \frac{1}{\rho_{gs}}\,(\frac{Q_k}{h_{fg}} - \frac{\dot{p}}{h_{fg}}(V_g(\rho_{gs}\,\frac{dh_{gs}}{dp_s} + h_{fg}\,\frac{d\rho_{gs}}{dp_s}) + V_f\rho_{fs}\,\frac{dh_{fs}}{dp_s} - V_s) - W_g) \qquad (6.2.9)$$

$$W_f = W_s - W_g + \dot{V}_g(\rho_{fs} - \rho_{gs}) - \dot{p}(V_g\,\frac{d\rho_{gs}}{dp_s} + V_f\,\frac{d\rho_{fs}}{dp_s}). \qquad (6.2.10)$$

As we need four output variables for the secondary side ($V_g$, $W_f$, $W_g$ and $a$), we must find a further two equations. One is obtained by use of the steam to water slip ratio S. For the other, an empirical relation, $F_a$, between the void volume $V_g$ and the outlet void fraction $a$, will be used.

$$W_g = S\,W_f\,\frac{a}{1-a}\,\frac{\rho_{gs}}{\rho_{fs}}, \qquad (6.2.11)$$

$$a = F_a\,(V_g)\,\frac{V_g}{V_s}\,. \qquad (6.2.12)$$

The equations for the riser, steam volume, and feed water chamber are in the basic form used as given in section 6.1:

$$\tau_r = \frac{1}{W_g}\,V_r\,a\,\rho_{gs}, \qquad (6.2.13)$$

$$\dot{a}_r = \frac{1}{\tau_r}\,(a - a_r), \qquad (6.2.14)$$

$$\dot{p} = (W_g - W_l - W_r\,\dot{a}_r\,\rho_{gs})/((V_e + a_{rm}\,V_r)\,\frac{d\rho_{gs}}{dp_s} + C1) \qquad (6.2.15)$$

$$C1 = \frac{1}{h_{fg}}\,(\rho_{fs}\,\frac{dh_{fs}}{dp_s}\,(V_{bh} + V_r - a_r V_r) + (V_e + a_{rm}V_r)(\rho_{gs}\,\frac{dh_{gs}}{dp_s} - 1)),$$

$$W_b = W_f + \dot{p}\,C1 + V_r\,\dot{a}_r\,\rho_{fs}, \qquad (6.2.16)$$

$$\dot{T}_b = \frac{1}{V_{bl}\rho_{fs}}\,(W_b(T_{sa} - T_b) - W_i(T_b - T_i)\,\frac{c_{pm}}{c_{ps}}). \qquad (6.2.17)$$

The downcomer is treated as one section giving a single time lag function.

$$\dot{T}_d = \frac{1}{V_d \rho_{fs}} W_s (T_b - T_d) . \qquad (6.2.18)$$

The basic equation for the friction calculation in the secondary side of the core is the same as in section 6.1, but the velocity v is taken as the water inlet velocity $v_{fi}$, and $\Delta R \Delta x$ is approximated by an empirical function $F_R$ of the void volume $V_g$. The equation then takes the following form:

$$\frac{\Delta p_1}{\rho_{fs}} = \frac{0.092}{De_s^{1.2}} F_f F_R v_{fi}^{1.8} . \qquad (6.2.19)$$

The pressure drop in the other part of the hydraulic loop and the circulation velocity is calculated just as in section 6.1.

$$\frac{\Delta p_2}{\rho_{fs}} = \frac{0.092}{De_d^{1.2}} F_f L'_a v_d^{1.8}, \qquad (6.2.20)$$

$$V_d = \frac{1}{\Sigma L_x A_d/A_x} \left( \frac{V_g}{A_s} g - \left( \frac{\Delta p_1}{\rho_{fs}} + \frac{\Delta p_2}{\rho_{fs}} \right) \right) , \qquad (6.2.21)$$

$$W_s = A_d v_d \rho_{fs} . \qquad (6.2.22)$$

The water level is finally given by:

$$\dot{L}_b = \frac{1}{A_b \rho_{fs}} \left( W_b + W_i - W_s - \dot{p} \frac{d \rho_{fs}}{d p_s} \Sigma V \right), \qquad (6.2.23)$$

where $\Sigma V$ is the sum of all water volumes outside the core.

Several coefficients in these equations will vary with temperature and pressure, but an analysis has shown that only few of them are important for the overall performance of the steam generator. Details of the analysis will not be included in the present report, only that three parameters were found so important that they must be calculated as functions of the temperature or pressure, these are: $c_{pp}$ in eq. (6.2.1a), $h_{fg}$ in equation (6.2.9), and $\rho_{gs}/\rho_{fs}$ in eq. (6.2.11). Variations in other parameters are of minor importance for the transient response of the main variables, even though



some have a considerable influence on the internal variables, especially in the short time scale.

The selection of the two empirical functions $F_a$ and $F_R$ is based upon static values calculated by the detailed model. The results are shown in fig. 12; two linear functions were used for $F_a$ and $F_R$.

The simplified model is realised as an analog version where the three variable coefficients mentioned above are inserted via MDAC units. The model has three output variables: primary outlet temperature, secondary steam pressure and water level, and four input variables: primary inlet temperature, feedwater temperature and flow, and steam load.

Transient responses for the two models are compared on figs. 13 and 14. The first figure shows the responses in steam pressure and primary outlet temperature for a step in steam valve opening; the next figure shows the same variables for a step in primary inlet temperature. In both cases the agreement for steam pressure is excellent. For the outlet temperature the deviation in the responses for the two models is quite clear, but still acceptable, especially as the simplified model will never be exposed to step change in the inlet temperature or other signals with high frequency components.

Symbols for the steam generator model

A : cross sections ($m^2$)

- $A_p$: core primary
- $A_s$: core secondary
- $A_r$: riser
- $A_b$: feed water chamber
- $A_d$: downcomer

De : hydraulic diameters (m)

- $De_p$: core primary
- $De_s$: core secondary
- $De_d$: downcomer

V : volumes ($m^3$)

- $V_p$: primary side
- $V_s$: secondary side

$V_e$: steam volume

$V_r$: riser

$V_{bl}$: feed water chamber below inlet

$V_{bh}$: feed water chamber above inlet

$V_{pi}$: primary inlet chamber

$V_{po}$: primary outlet chamber

$V_g$: total void volume in core

L : length (m)

$L_b$: feed water chamber (water level)

$L_r$: riser

$L_d$: downcomer

$L_c$: core

$$\Delta x = \frac{L_c}{20}$$

$$\Delta z = \frac{L_c}{20}$$

$\Delta r$ : tube thickness

0 : Surfaces ($m^2/m$) for one flow direction

$O_p$: core primary

$O_s$: core secondary

$O_r$: core tube between inside and outside shell

G : mass flow per $m^2$ ($kg/s\ m^2$)

W : mass flow (kg/s)

$W_p$: core primary

$W_s$: core secondary inlet

$W_g$: core secondary steam phase

$W_f$: core secondary water phase

$W_{go}$: core secondary steam outlet

$W_{fo}$: core secondary water outlet



$W_l$: steam load

$W_i$: feed water inlet

$W_b$: water to feed water chamber

T : Temperature ($^oC$)

$T_p$: core primary

$T_s$: core secondary

$T_{r1}$: core tube wall inside

$T_{r2}$: core tube wall outside

$T_b$: feed water chamber

$T_d$: downcomer

$T_{pi}$: primary inlet

$T_{po}$: primary outlet

$T_{p1}$: primary inlet chamber

$T_{p2}$: primary outlet chamber

$T_{si}$: core secondary inlet

$T_{sa}$: saturation

q : Heat flow per m (MW/m)

$q_p$: from primary flow

$q_s$: to secondary flow

$q_r$: through tube wall

Q : Heat flow (MW)

$Q_p$, $Q_s$ and $Q_r$ correspond to $q_p$, $q_s$ and $q_r$

$Q_k$: heat flow for steam production

v : Velocities (m/s)

$v_f$: core water phase

$v_g$: core steam phase

$v_{go}$: core steam outlet

$v_d$: downcomer

h : Enthalpy (MJ/kg)

$h_i$: feed water inlet

$h_b$: feed water chamber

$h_{gs}$: saturated steam

$h_{fs}$: saturated water

$h_{fg} = h_{gs} - h_{fs}$ evaporation heat

$\rho$ : Densities ($kg/m^3$)

$\rho_f$: water

$\rho_g$: steam

$\rho_{gs}$: saturated steam

$\rho_{fs}$: saturated water

$c_p$ : Heat capacities

$c_{pp}$: primary specific (MJ/kg $^oC$)

$c_{ps}$: secondary specific (MJ/kg $^oC$)

$c_{pi}$: feed water inlet specific (MJ/kg $^oC$)

$c_{pm}$: $1/2(c_{ps} + c_{pi})$ (MJ/kg $^oC$)

$C_r$: tube wall (MJ/m $^oC$)

$\alpha$ : Void fraction

$\alpha_o$: core outlet

$\alpha_r$: riser

$\alpha_m$: mean void fraction in core

$\alpha_{rm}$: mean void fraction in riser

$\eta$: Dynamic viscosity (kg/m s)

$\lambda_r$: Thermal conductivity for U-tube (MW/m $^oC$)

f: Single-phase friction coefficient

$F_f$: Single-phase friction parameter

R: Two-phase friction multiplier

$R_e$: Reynolds number



H: Heat transfer parameter

S: Slip factor = $v_g/v_f$

X: Steam quality

p: Steam pressure (bar)

$C_l$: Steam load constant (kg/s bar)

g: Gravitation constant ($m/s^2$)

## 7. THE TURBINE-REHEATER MODEL

### 7.1. Pressure and Flow Calculations

A steam flow diagram is shown in fig. 15. It is assumed that the steam flows from the main steam line through the regulating valve to the HP inlet steam chamber, with volume $V_h$, further through the HP turbine to the moisture separator and reheater, with volume $V_l$, and then through the LP turbine to the condenser. From the HP turbine a fixed fraction $a_h$ goes to feed water reheaters, and a variable fraction $a_t$ is separated as water in the moisture separator.

The pressure dynamics is related to the two volumes $V_h$ and $V_l$ and is calculated by steam mass balance equations:

$$\dot{p}_h = \frac{1}{V_h \frac{d\rho_{gs}}{dp_s}} (G_v - G_h) . \qquad (7.1)$$

$$\dot{p}_l = \frac{1}{V_l \left(\frac{\partial \rho_g}{\partial p}\right)_h}, \qquad G_r = (1 - a_t)G_t . \qquad (7.2)$$

Steam flows are calculated using the general flow equation for subsonic flow through convergent - divergent ducts:

$$G = \text{const.} * A \left[2g \frac{k}{k-1} \frac{p}{v} \left(r^{\frac{2}{k}} - r^{\frac{k+1}{k}}\right)\right]^{0.5} ,$$

where K is the ratio of specific heats $c_p/c_v$, r is the outlet-inlet pressure ratio, p is the inlet pressure and v the corresponding specific steam volume. A is the flow area and g the gravitation constant.

The formula can be written as

$$G = \text{const.} * A\ Y\ \left(\frac{p}{v}\right)^{0.5}$$

$$Y = 2g\frac{k}{k+1}\left(r^{\frac{2}{k}} - r^{\frac{k+1}{k}}\right)^{0.5}$$

For the pressure range up to 80 bar the density for saturated steam is roughly proportional to the pressure. Use of this relation reduces the flow formula to:

$$G = \text{const.} * A\ Y\ p$$

This formula will also be used for the LP turbine even though the inlet steam is superheated, because the superheating is small and is only valid for the first third of the LP stage.

When the pressure ratio is below the critical value (here 0.577), the flow velocity is equal to the sonic velocity and the mass flow is independent of the pressure ratio. The normalized function Y for k = 1.135 is shown in fig. 16.

For the regulating value the pressure ratio will vary in the range from 0.95 at full load to 0.1 at minimum load, so the flow equation is used as:

$$G_v = k_v\, A_v\, p_v\, Y_v\, (p_v/p_h)\,, \tag{7.3}$$

where $A_v$ is normalized valve opening area and $Y_v$ is the normalized function in fig. 16.

For the HP turbine the pressure ratio is about 0.25 at all loads, so Y is constantly equal to 1. The flow equation is then:

$$G_h = k_h\, p_h\,. \tag{7.4}$$

The conditions are more complicated for the LP turbine. For the first stages the pressure ratio is nearly constant giving the same simple expression as eq. (7.4), but for the last stage the pressure ratio changes with load. However, as the last stage is normally designed for near critical flow, and the value of Y for the other stages is nearly constant, the same simple relation will be a useful approximation.

$$G_l = k_l\, p_l\,. \tag{7.5}$$

A more accurate calculation would also require a more detailed description



third-order polynomials in the saturation temperature, which again is calculated by a fourth-order polynomial in the pressure.

## 7.3. Reheater Calculations

A schematic diagram of the simplified reheater model is shown as part of fig. 15. The hot steam flowing through the tubes is completely condensed before it leaves the reheater at saturation temperature. It is assumed that the water level at the bottom is controlled automatically. The secondary steam in the reheater mainly flows in cross flow and will be in a superheated condition all the time.

The heat transfer is described by a constant temperature drop from the hot steam to the water film on the tubes and constant heat transfer coefficients for the tube wall on the two sides of the tubes. All the tube heat capacity is concentrated on the cold side of the tube (between two heat transfer coefficients). The secondary temperature is calculated by the energy balance equation assuming equal temperature all over the volume.

The equations are:

$$T_{t1} = T_{sa} - \Delta T_{t1} \tag{7.21}$$

$$Q_t = k_t(T_{t1} - T_{t2}) \tag{7.22}$$

$$Q_r = k_r(T_{t2} - T_{ro}) \tag{7.23}$$

$$\dot{T}_{t2} = \frac{1}{C_t}\,(Q_t - Q_r) \tag{7.24}$$

$$\dot{T}_{ro} = \frac{1}{V_r \rho_g c_p}\,(Q_r - G_r\, c_p\,(T_{ro} - T_{ri})) \tag{7.25}$$

$$G_m = \frac{Q_r}{h_{fg}}\,. \tag{7.26}$$

The coefficients $k_t$ and $k_r$ are fixed heat transfer coefficients calculated from basic heat transfer data and full load working values. $\Delta T_{t1}$ is a fixed temperature drop on the primary side of the tubes.

## 7.4. Implementation of the Model

The equations are solved by hybrid calculations. The pressure and the heat transfer dynamics are solved by analog components, while the power calculation is carried out digitally. The digital routine reads the pressures and the heat flow to the secondary side of the reheater from the

analog machine. The turbine module obtains the inlet steam pressure and saturation temperature from the steam generator module, and as output gives the steam load ($G_v + G_m$) and the electrical power $E_g$. Internal variables as pressures and reheater temperatures may be investigated during transients. The steam and water drain from the HP and LP turbines is not used, since no feedwater model is included in the station model.

Symbols for the turbine-reheater model

| | | |
|---|---|---|
| p | : Pressure | bar |
| G | : Flow | kg/s |
| T | : Temperature | $^oC$ |
| Q | : Heat flow | MW |
| E | : Power | MW |
| V | : Volume | $m^3$ |
| ρ | : Density | $kg/m^3$ |
| h | : Enthalpy | MJ/kg |
| S | : Entropy | MJ/kg K |
| c | : Heat capacity, specific | MJ/kg $^oC$ |
| C | : Heat capacity | MJ/kg |
| X | : Steam quality | |

Indices

| | |
|---|---|
| h | : HP-turbine |
| l | : LP-turbine |
| v | : Regulating value |
| c | : Condenser |
| t | : Moisture separator |
| r | : Reheater |
| sa | : Saturation |
| gs | : Saturated steam |
| fs | : Saturated water |



t, $t_1$, $t_2$ : Tube in reheater, hot/cold side

r, ri, ro : Reheater, inlet/outlet

## 8. THE ELECTRICAL POWER GRID

The nuclear power station is assumed to supply power to an electrical grid in parallel with one other major power station. The relative power contribution from the two stations is $E_1/E_n$ and $E_2/E_n$. The power grid itself is represented by a single time lag function derived below. The other power station is assumed to be equipped with a frequency controller with proportional-integral control. The nuclear station itself is controlled by a power controller in the present basic version.

The grid is characterised by two quantities: the total kinetic energy $K_e$ of the rotating machines, and the grid frequency characteristic droop $S_a$ defined as $\Delta E/\Delta f$, where $\Delta E$ and $\Delta f$ are small deviations from the steady state in power and frequency. The grid frequency characteristic droop $S_a$ is a measure for the change in power consumption during frequency deviations.

A change in power production $\Delta E_o$ without frequency control in the system results in a steady state deviation in frequency $\Delta f = \Delta E_o/S_a$. The transient is governed by a first-order differential equation derived from the fundamental equation for a rotating machine

$$J \cdot \dot{\omega} = M .$$

Insertion of $\omega = 2\pi f$, $K_e = \frac{1}{2} J \omega_n^2$ and $\Delta E = M \cdot \omega_n$ leads to:

$$\dot{f} = \frac{\Delta E}{2 K_e} f_n . \qquad (8.1)$$

The term $\Delta E$ is the deviation between power production and consumption. Following a step change $\Delta E_o$, $\Delta E$ will decrease towards zero as:

$$\Delta E = \Delta E_o - \Delta f \; S_a .$$

Insertion in 8.1 and normalising with $f_n$ gives:

$$\frac{\dot{\Delta f}}{f_n} = \frac{f_n}{2 K_e} \left( \frac{\Delta E_o}{f_n} - S_a \frac{\Delta f}{f_n} \right) , \qquad (8.2)$$

and solution of 8.2 gives:

$$\frac{\Delta f}{f_n} = \frac{\Delta E_o}{f_n S_a}(1 - e^{-t/\tau}); \qquad \tau = \frac{2 K_e}{f_n S_a} . \tag{8.3}$$

The quantities $S_a$ and $K_e$ are roughly proportional with the size of the grid, while the time constant $\tau$ only depends on the type of load on the grid. Introduction of the relative grid frequency characteristic droop $S_r = S_a f_n/E_n$ gives a form of equation (8.2) which is independent of the grid size.

$$\frac{\Delta f}{f_n} = \frac{1}{\tau}\left(\frac{1}{S_r}\frac{\Delta E}{E_n} - \frac{\Delta f}{f_n}\right) . \tag{8.4}$$

As the equations in the present chapter are all linear, the differential equations are most conveniently expressed by means of the Laplace operator s. This gives the final form of the grid equation:

$$\frac{\Delta f}{f_n} = \frac{\Delta E}{E_n}\frac{1/S_r}{1 + s\tau} . \tag{8.5}$$

The equation for the power station with frequency control is taken as:

$$\frac{\Delta E_2}{E_2} = \frac{\Delta f}{f_n}\left(\frac{1}{\delta_2} + \frac{k_{e2}}{s}\right)\frac{1}{(1 + \tau_{2v}s)(1 + \tau_{2t}s)} . \tag{8.6}$$

The equation gives the variation in power production caused by variations in the frequency. The normalization is used to make the equation independent of the grid size. The two terms, $\frac{1}{\delta_2}$ and $k_{e2}$, are the proportional and the integral gains of the controller. The time constants, $\tau_{2v}$ and $\tau_{2t}$, belong to the steam valve and the turbine generator unit. The steam valve speed signal is limited, corresponding to the working time from open to closed valve. The representation used here is a very rough approximation giving only the fundamental characteristics of the generating units, nevertheless it is sufficient for the purpose.

The deviation between power production and consumption, $\Delta E$, may be calculated as:

$$\frac{\Delta E}{E_n} = \frac{E_2}{E_n}\frac{\Delta E_2}{E_2} + \frac{1}{E_n}\Delta E_1 + \frac{\Delta E_1}{E_n} . \tag{8.7}$$

In the basic version the nuclear power station itself is equipped with a power controller with integral action between power deviations and the



opening of the steam valve:

$$\dot{A}_v = k_{e1}(E_1 - E_{1r}) . \tag{8.9}$$

The steam valve speed signal $A_v$ is limited as it is in the other stations.

The model of the power grid is realised as a wholly analog model consisting of linear computing elements only.

Symbols for the power grid

$E_1$ : Power from the nuclear station, equal to $E_g$ in chapter 7

$E_{1r}$ : Reference value for $E_1$

$E_2$ : Power from all other stations

$E_n$ : Nominal grid power

$\Delta E_1$ : Variation in load power

$f$ : Grid frequency

$f_n$ : Nominal grid frequency

$J$ : Moment of inertia

$\omega$ : Angular frequency

$M$ : Torque

$K_e$ : Kinetic energy of all rotating machines at the grid

$S_a$ : Grid frequency characteristic droop

$S_r$ : Relative grid frequency characteristic droop

$\tau$ : Time constant of the grid

$\tau_{2v}$ : Time constant of steam valves

$\tau_{2t}$ : Time constant of turbines

$\delta_2$ : Proportional band for frequency controller

$k_{e2}$ : Integration gain of frequency controller

$k_{e1}$ : Gain of the power regulator for the nuclear station

REFERENCE

P. la Cour Christensen: User's Manual for the PWR-PLASIM Model. Risø-M-1757 Report (1975).

## APPENDIX A

The hybrid computer configuration:

1. An EAI 680 analog computer with:

30 integrators
12 track-store summer amplifiers
12 limit summer amplifiers
12 special function generators with junction inverters
6 junction inverters
42 inverter amplifiers
24 multipliers
24 DA/AD interface units with junction inverters
12 adjustable diode function generators
132 coefficient potentiometers
Various logical units
All junction inverters may be used as summing amplifiers

A PDP8 computer with:

12 k core memory
A 800 k disk memory
A floating point hardware processor
A dual DEC tape unit

The interface system between the two machines consists of:

24 AD conversion channels
8 DA converters
24 multiplying DA converters
12 digital inputs
12 digital outputs



## APPENDIX B

Basic continuity equations for mass, energy and momentum.

For a one-dimensional flow of a single phase with flow area A, the mass and energy equations are:

$$\frac{\partial \rho}{\partial t} = - \frac{\partial G}{\partial x} \qquad (B1)$$

$$\frac{\partial (\rho u)}{\partial t} = \frac{q}{A} - \frac{\partial (Gu)}{\partial x} - \frac{\partial (G p v)}{\partial x} \qquad (B2)$$

G: Flow rate per unit area
u: Internal energy
q: Heat flow per unit length
$\rho$: Density
v: Specific volume

Introduction of the enthalpy $h = u + pv$ simplifies equation B2:

$$\frac{\partial (\partial h)}{\partial t} - \frac{\partial p}{\partial t} = \frac{q}{A} - \frac{\partial (Gh)}{\partial x} \qquad (B3)$$

Combination of equations B1 and B3 as B3 - h * B1 lead to the final form of the energy equation:

$$\rho \frac{\partial h}{\partial t} = \frac{q}{A} - G \frac{\partial h}{\partial x} + \dot{p} \qquad (B4)$$

For a compartment with volume V, inlet flow $W_i$, outlet flow $W_o$ and complete mixing, the equations B1 and B4 take the following form:

$$\dot{\rho} = \frac{1}{V} (W_i - W_o) \qquad (B1a)$$

$$\dot{h} = \frac{1}{V\rho} (Q - W_i(h-h_i) + V\dot{p}) . \qquad (B4a)$$

For a single phase flow of subsaturated water the equations may be further reduced. As $\rho$ is nearly independent of pressure $\dot{\rho}$ will be nearly zero, so B1a vanishes. For B4a, h may be expressed as $c_p T$, where the heat capacity $c_p$ is a slowly varying parameter, so $\dot{c}_p \simeq 0$. Further, the

term $V\dot{\rho}$ is normally small compared with the other terms so it can be neglected. This reduces B4a to

$$\dot{T} = \frac{1}{V\rho}\left(\frac{Q}{c_p} - W(T-T_i)\right) . \qquad \text{(B4b)}$$

For a two-phase flow of water and steam in saturated condition, the following mass and energy equations may be used:

$$\frac{\partial}{\partial t}(\alpha \rho_{gs} + (1-\alpha)\rho_{fs}) = - \frac{\partial}{\partial x}(\rho_{fs} v_f (1-\alpha) + \rho_{gs} v_g \alpha) , \qquad \text{(B5)}$$

$$\frac{\partial}{\partial t}(\alpha \rho_{gs} h_{gs} + (1-\alpha)\rho_{fs} h_{fs}) = \frac{q}{A} - \frac{\partial}{\partial x}(\rho_{fs} v_f (1-\alpha) h_{fs} + \rho_{gs} v_g \alpha h_{gs}) + \dot{p} . \qquad \text{(B6)}$$

Equations B5 and B6 are combined as B6 - $h_{fs}$ * B5, which leads to the reduced form:

$$(1-\alpha)\rho_{fs}\frac{\partial h_{fs}}{\partial t} + \alpha \rho_{gs}\frac{\partial h_{gs}}{\partial t} + h_{fg}\frac{\partial}{\partial t}(\alpha \rho_{gs}) =$$

$$\frac{q}{A} - h_{fg}\frac{\partial}{\partial x}(\rho_{gs} v_g \alpha) - \rho_{fs} v_f (1-\alpha)\frac{\partial h_{fs}}{\partial x} - \rho_{gs} v_g \alpha \frac{\partial h_{gs}}{\partial x} + \dot{p} \qquad \text{(B7)}$$

$h_{fg}$ is the evaporation heat.

For normal operating conditions the pressure and temperature variation along the channel will be small so the space derivative of h and $\rho$ can be neglected. This leads to the two equations used in chapter 6:

$$\frac{\partial}{\partial x}(v_f(1-\alpha)) = \dot{\alpha}\left(1 - \frac{\rho_{gs}}{\rho_{fs}}\right) - \dot{p}\left(\frac{\alpha}{\rho_{fs}}\frac{\partial \rho_{gs}}{\partial p} + \frac{1-\alpha}{\rho_{fs}}\frac{\partial \rho_{fs}}{\partial p}\right) - \frac{\rho_{gs}}{\rho_{fs}}\frac{\partial}{\partial x}(v_g \alpha) \qquad \text{(B5a)}$$

$$\frac{\partial}{\partial x}(v_g \alpha) = \frac{1}{h_{fg}\rho_{gs}}\left(\frac{q}{A} - \dot{p}\left(\alpha\left(\rho_{gs}\frac{\partial h_{gs}}{\partial p} + h_{fg}\frac{\partial \rho_{gs}}{\partial p}\right) + (1-\alpha)\rho_{fs}\frac{\partial h_{fs}}{\partial p} - 1\right)\right) - \dot{\alpha} \qquad \text{(B7a)}$$



The basic momentum equation is

$$\frac{\partial G}{\partial t} = - \frac{\partial U}{\partial x} - \frac{\partial p}{\partial x} - \frac{\partial F}{\partial x} + g \cos\varphi \cdot \rho_m \qquad \text{(B8)}$$

G: Mass flow per unit area
U: Momentum Flow per unit area
F: Friction force per unit area and length
g: Gravity constant
$\varphi$: Angle between flow direction and the gravity vector
$\rho_m$: Mean density

The momentum equation is only used to calculate the flow rate in closed circulation loops. For this purpose B8 is integrated along a closed loop; the result can be written as:

$$\frac{dJ}{dt} = D - \Delta p_f - L \qquad \text{(B9)}$$

J: Total momentum per unit area in the loop
D: Driving pressure derived from density differences and from pumps
$\Delta p_f$: Pressure drop from friction forces
L: Momentum losses at input, output and cross section restrictions

For a system with two-phase flow J and D is given by:

$$J = \oint (v_f \rho_f (1-\alpha) + v_g \rho_g \alpha)\, dx$$

$$D = g \oint \cos\varphi\, (\rho_f (1-\alpha) + \rho_g \alpha)\, dx + \Delta p_{pump} .$$

Normally the term L cannot be calculated explicitly but may sometimes be estimated by empirical expressions.

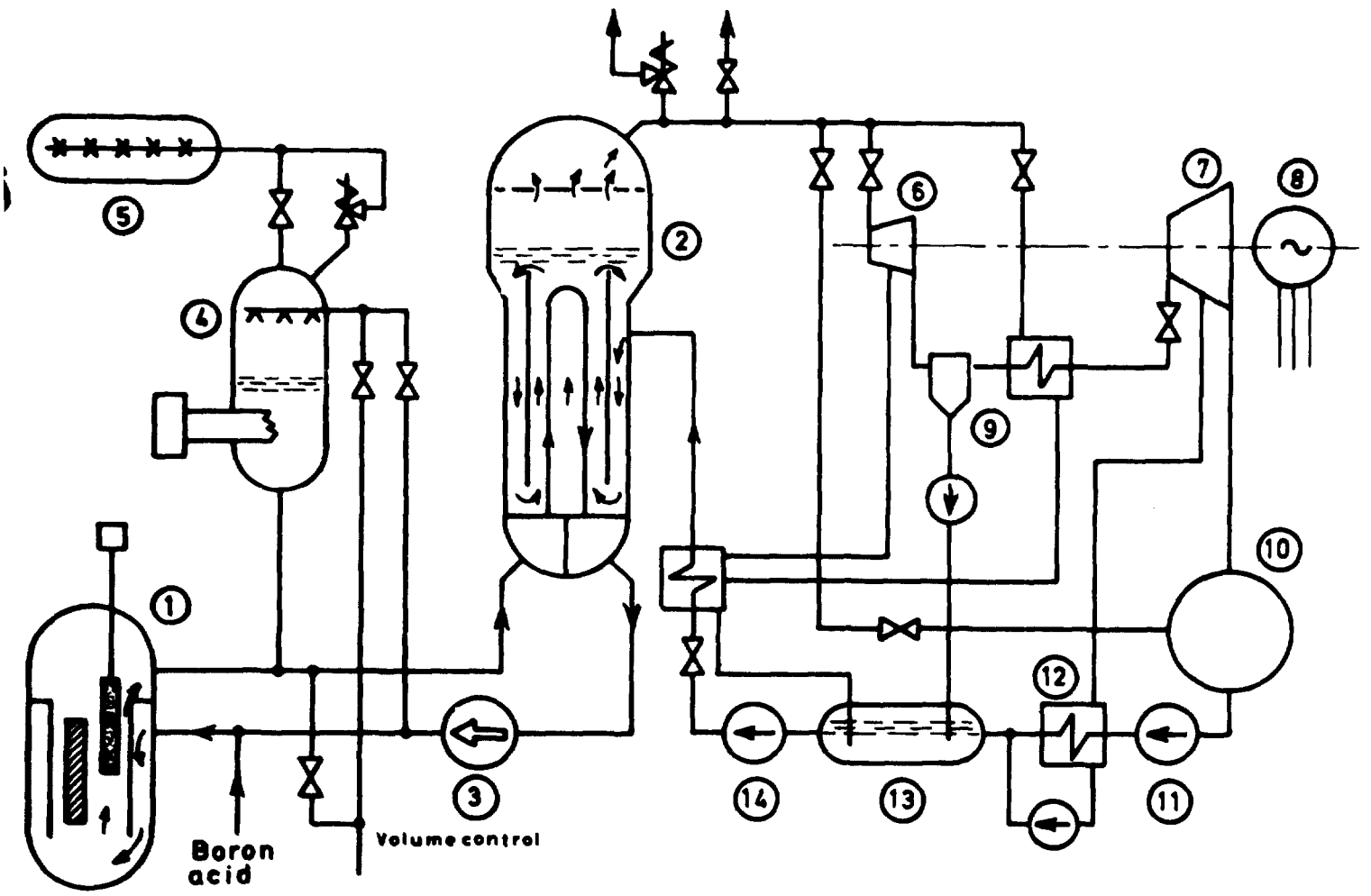


Fig. 1 PWR station flow diagram showing the main components in the primary and secondary loops. The model of the secondary side is simplified by omission of the preheaters, the condenser and the feedwater tank.



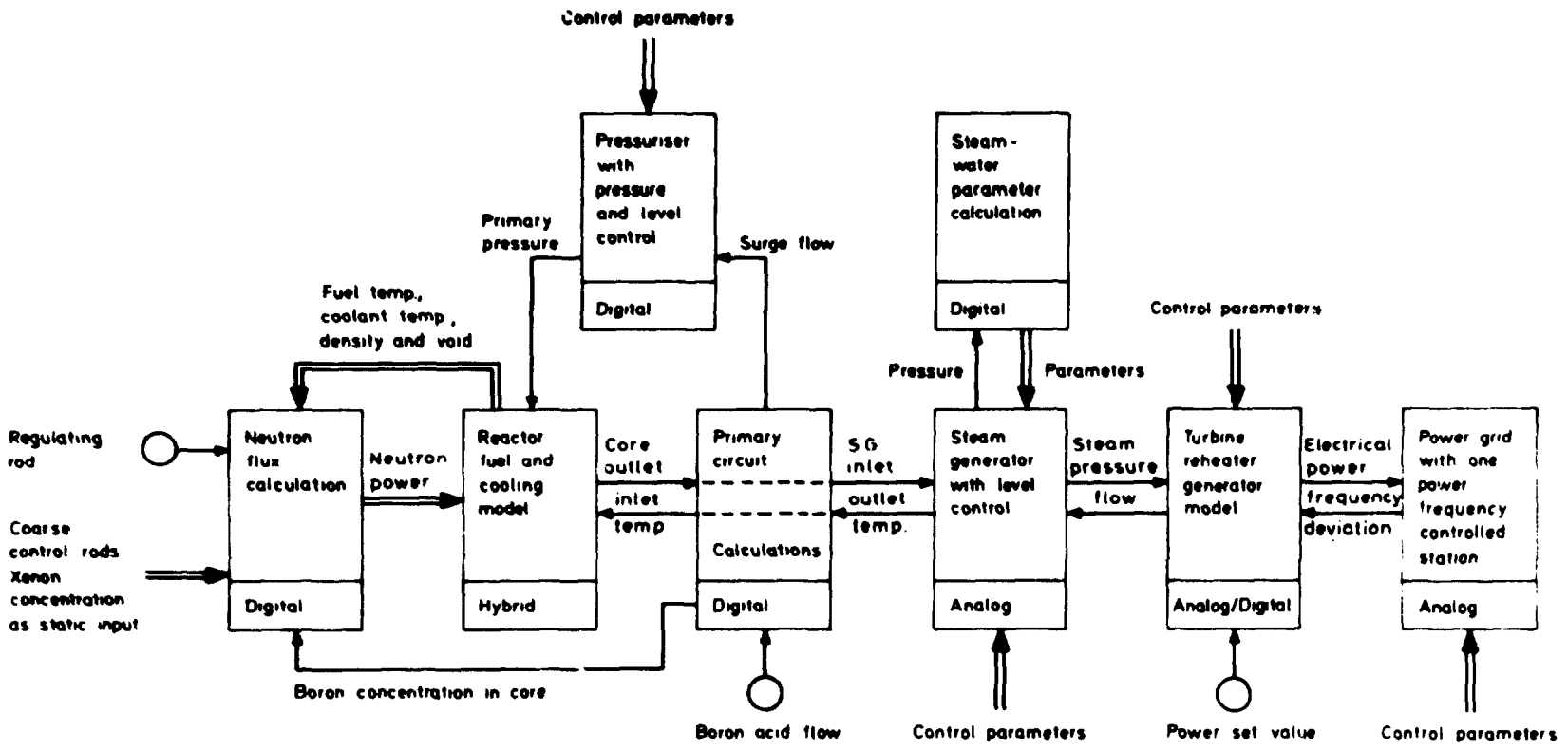


Fig 2 Diagram of PWR power station model

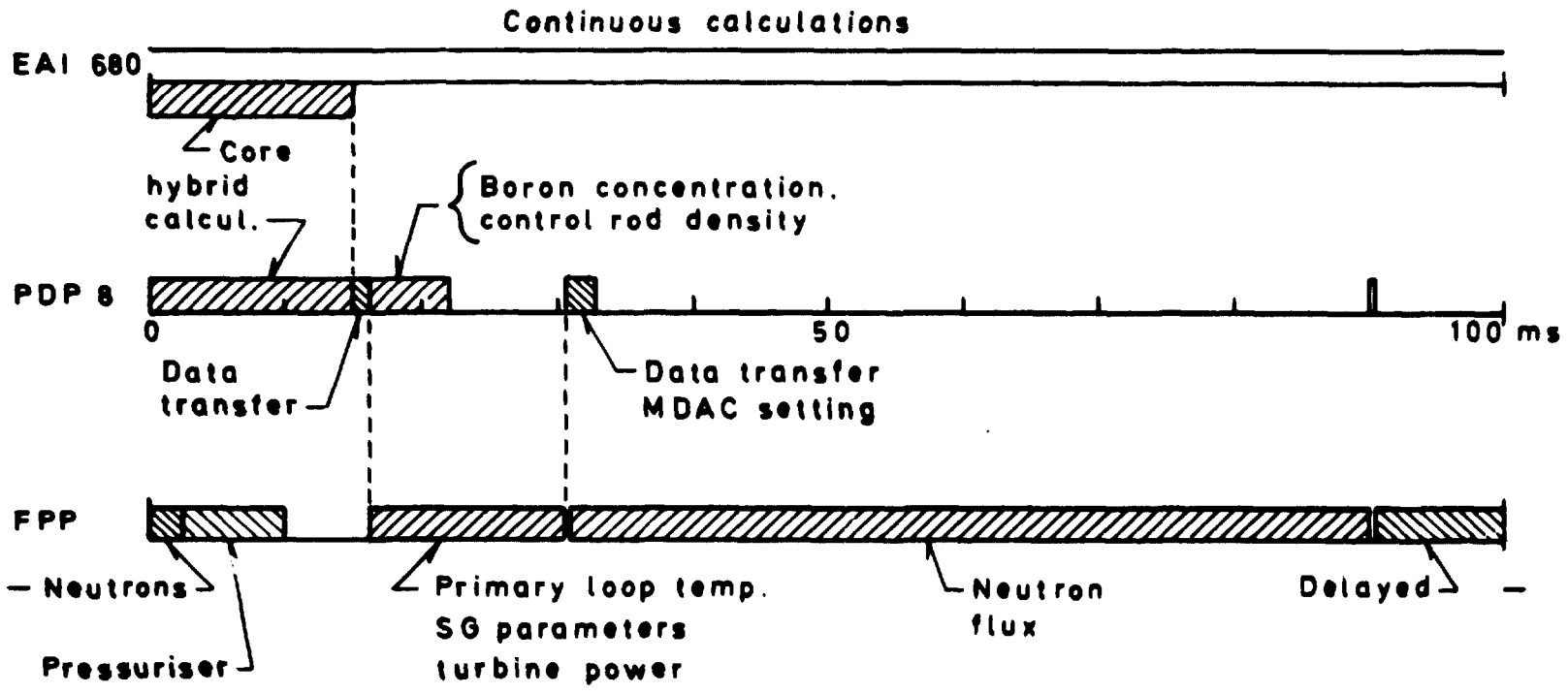


Fig.3. Job distribution diagram.



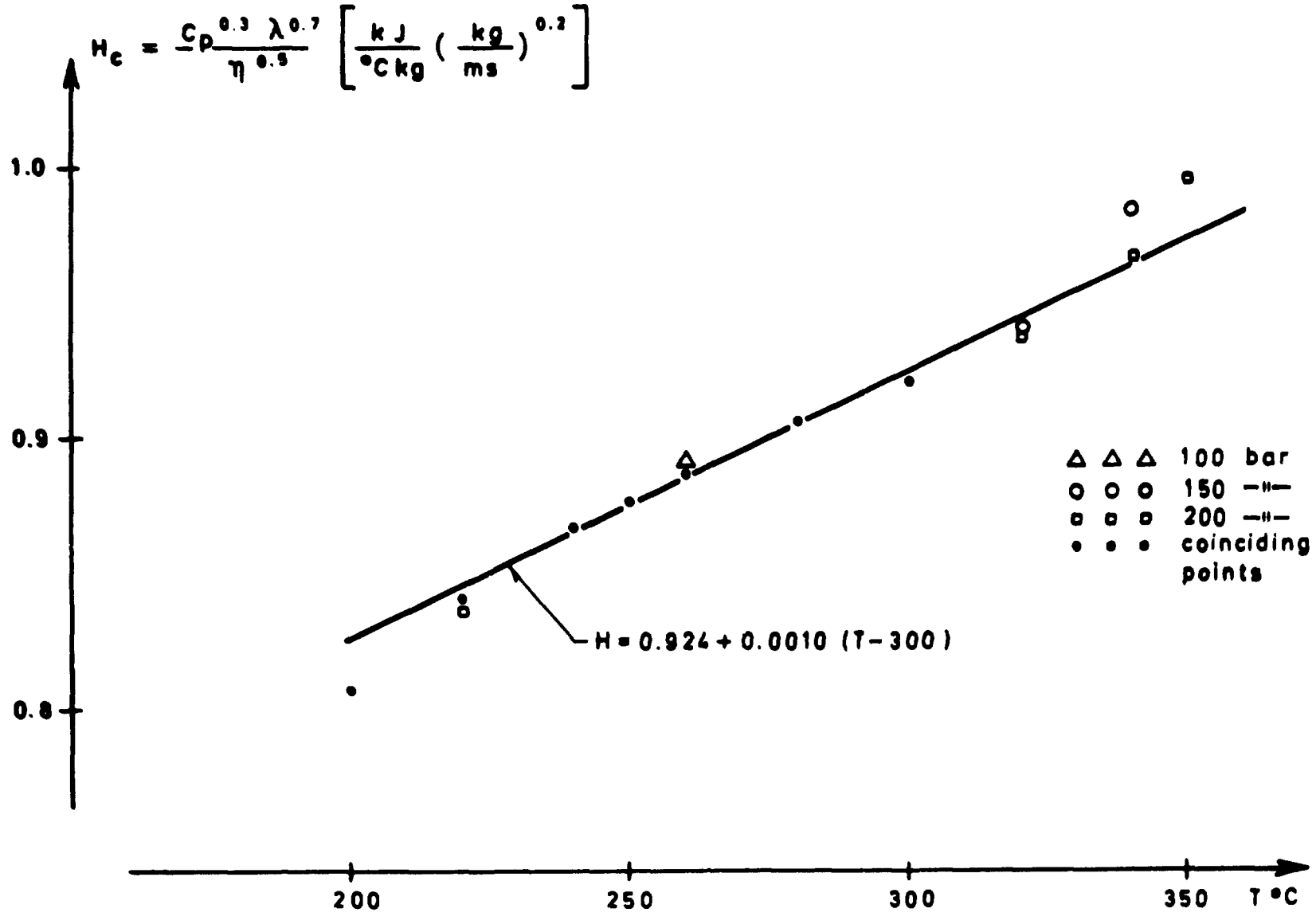


Fig.4. Heat transfer parameter $H_c(T)$ for the reactor core.

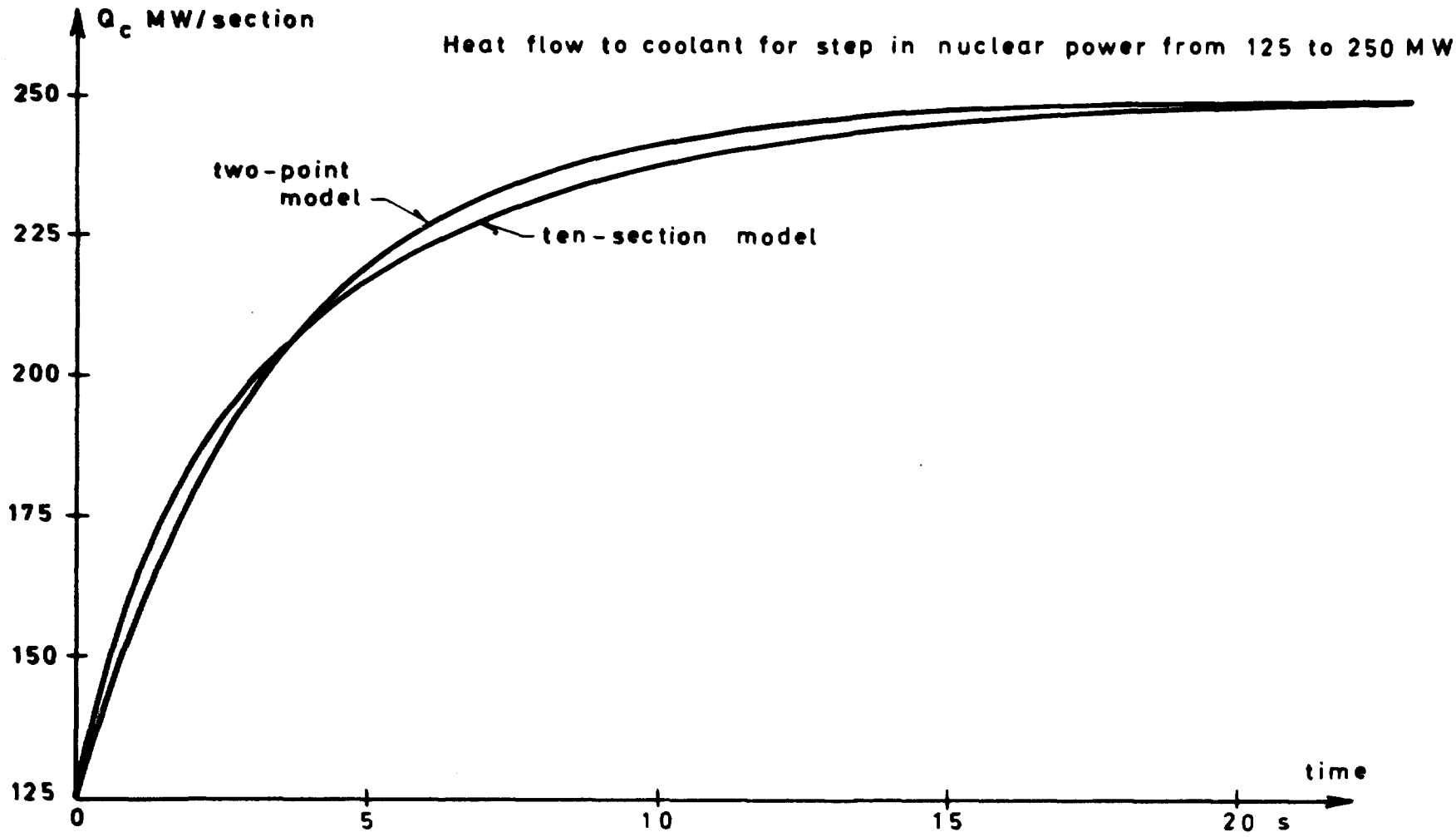


Fig.5. Comparison of step responses for the ten-section and the two-point fuel models.

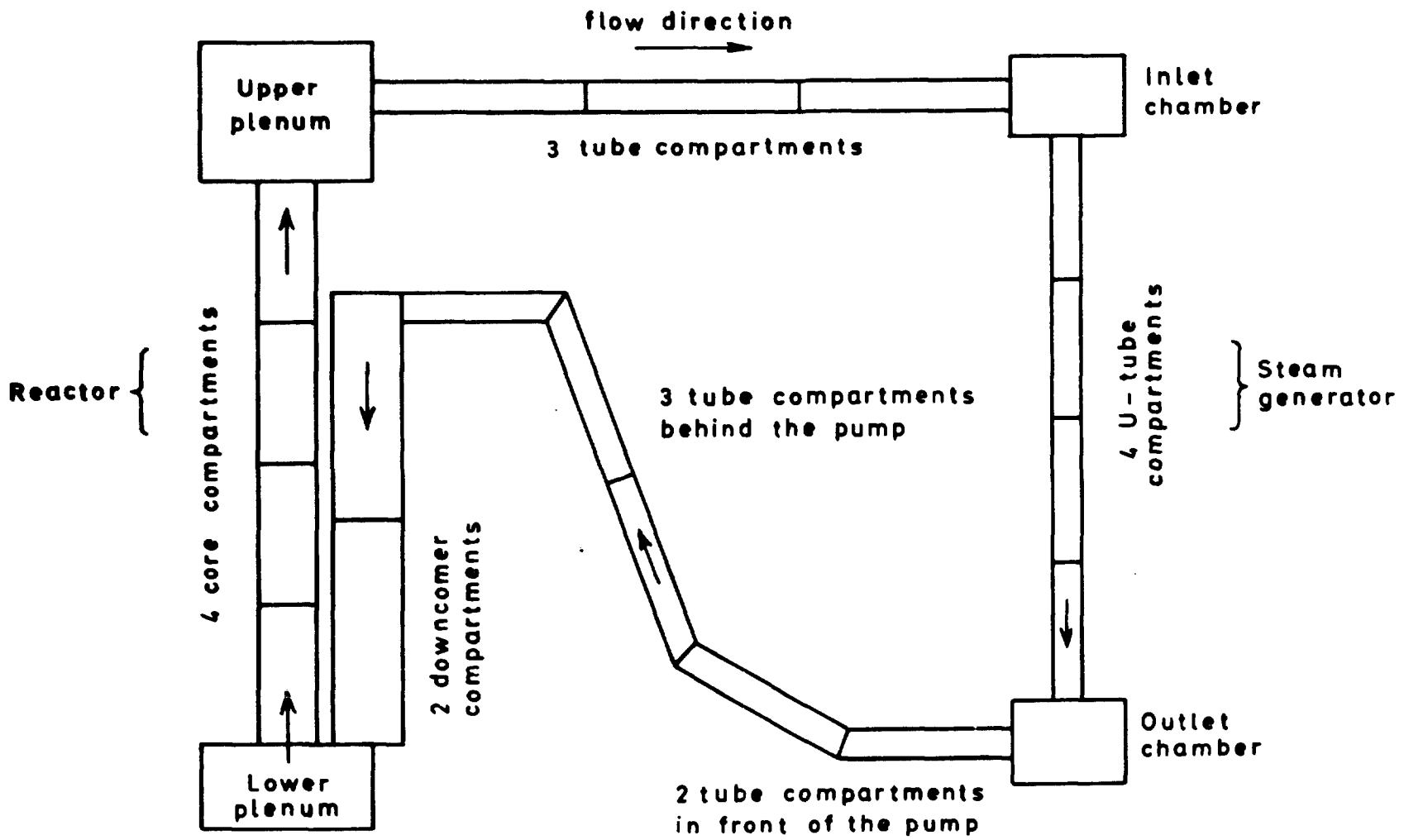


Fig. 6. Primary loop compartments for calculation of temperature and boron acid distribution.

Fig. 7. Comparison of transient response for the two pressuriser models

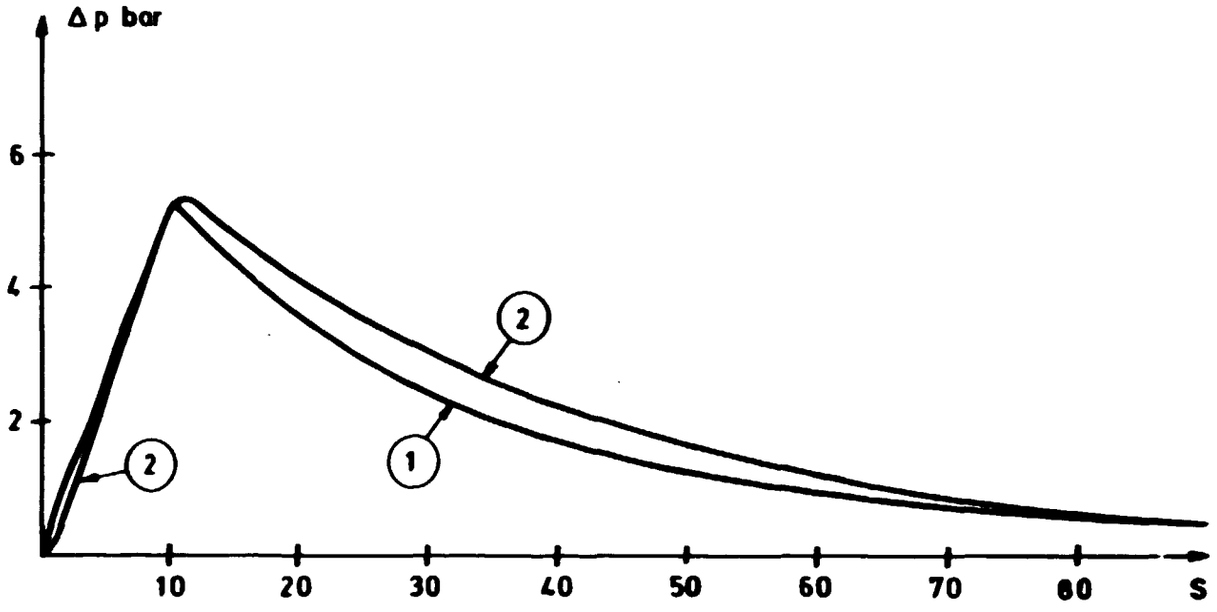


Transient response for an inlet flow impulse of 50 kg/s in 10 s.

1. The detailed model with steam superheating and heat transfer to the steel wall
2. The simplified model without steam superheating and heat transfer to the steel wall, but with a digital filter with a time lag of 0.5s in the inlet flow.



Fig. 8. Simplified diagram of U-tube steam generator

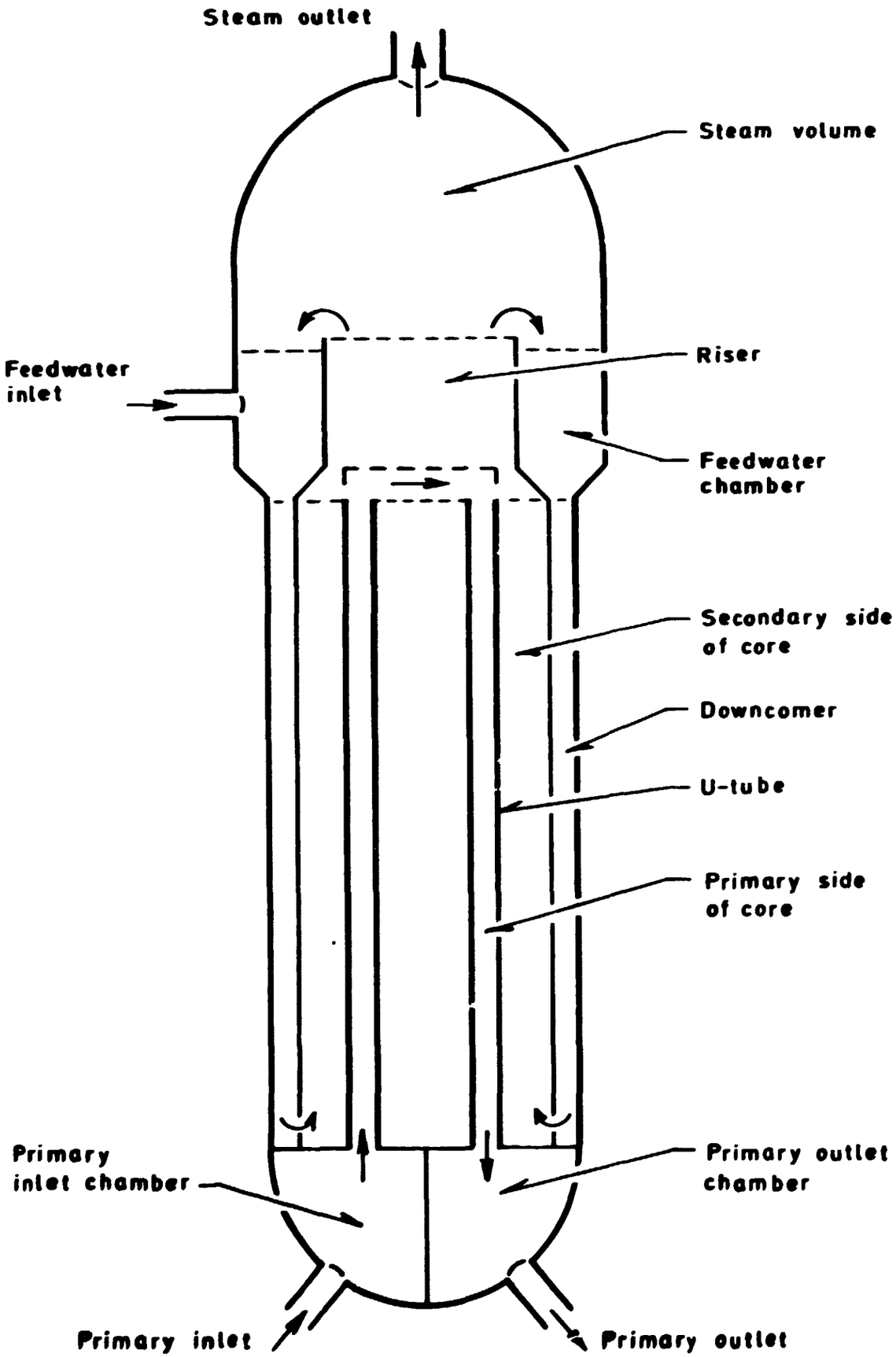

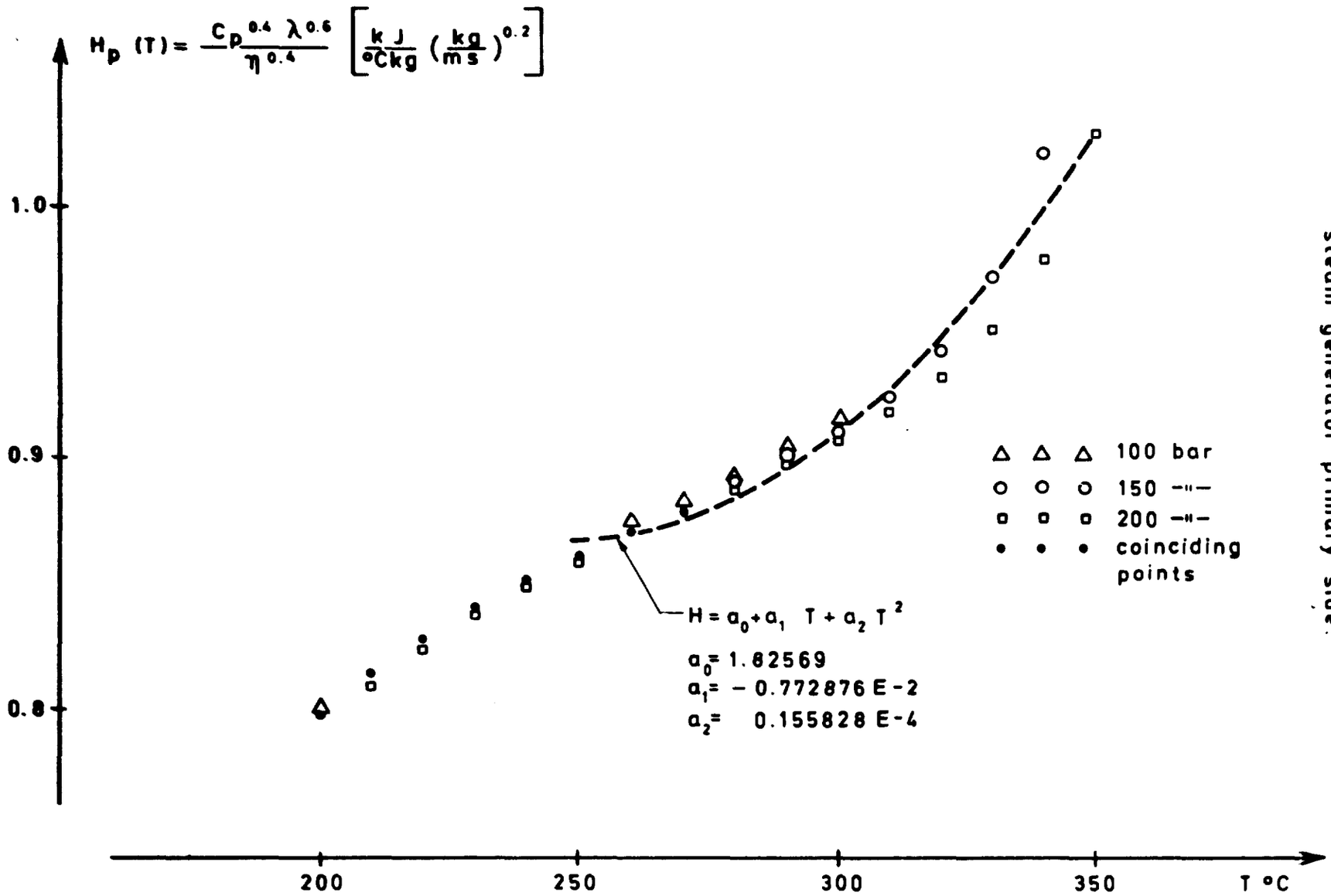


Fig. 9. Heat transfer parameter $H_p(T)$ for the steam generator primary side.



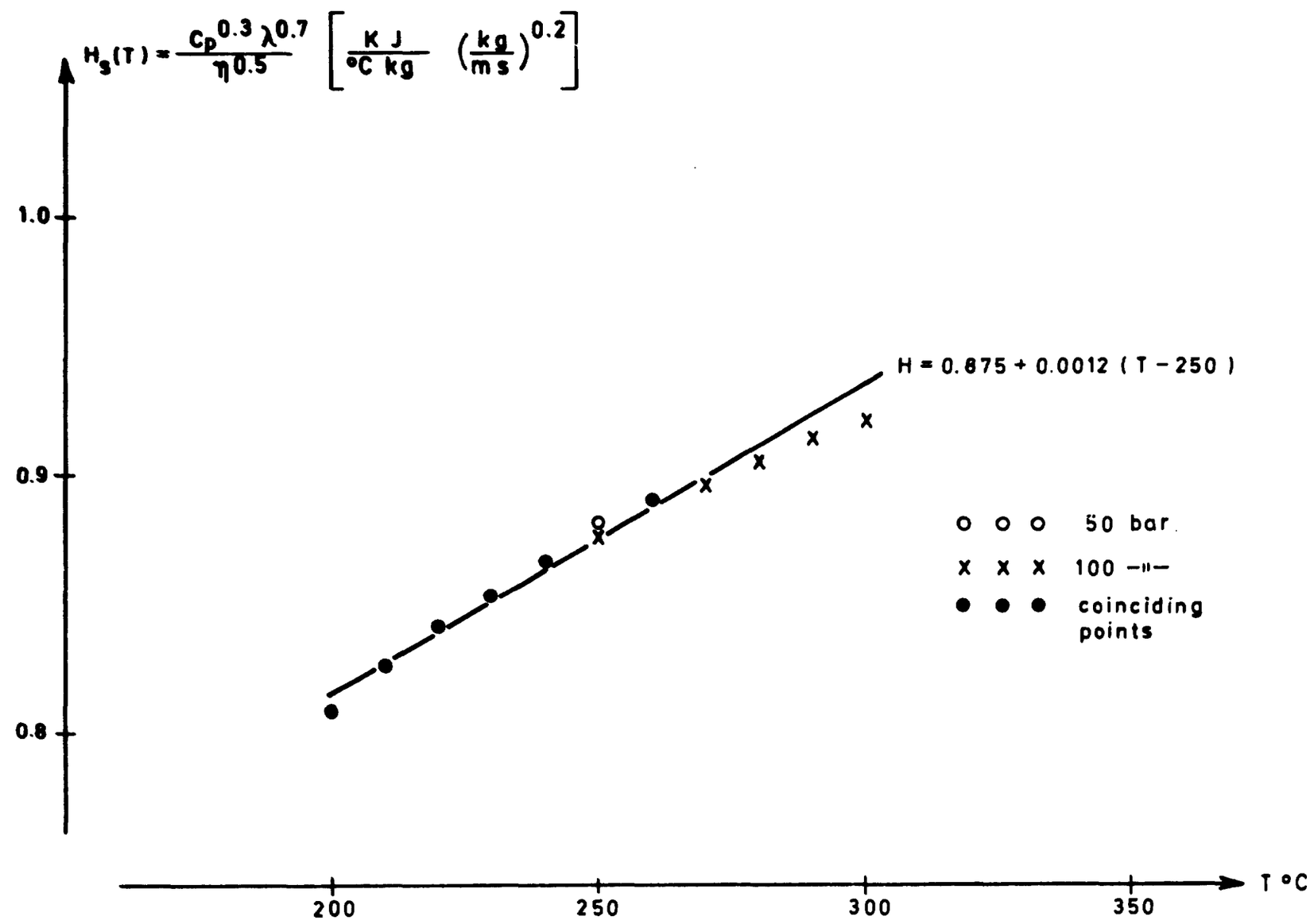


Fig. 10. Heat transfer parameter $H_s(T)$ for the steam generator secondary side

Fig. 11. The friction parameter $F_f(T)$

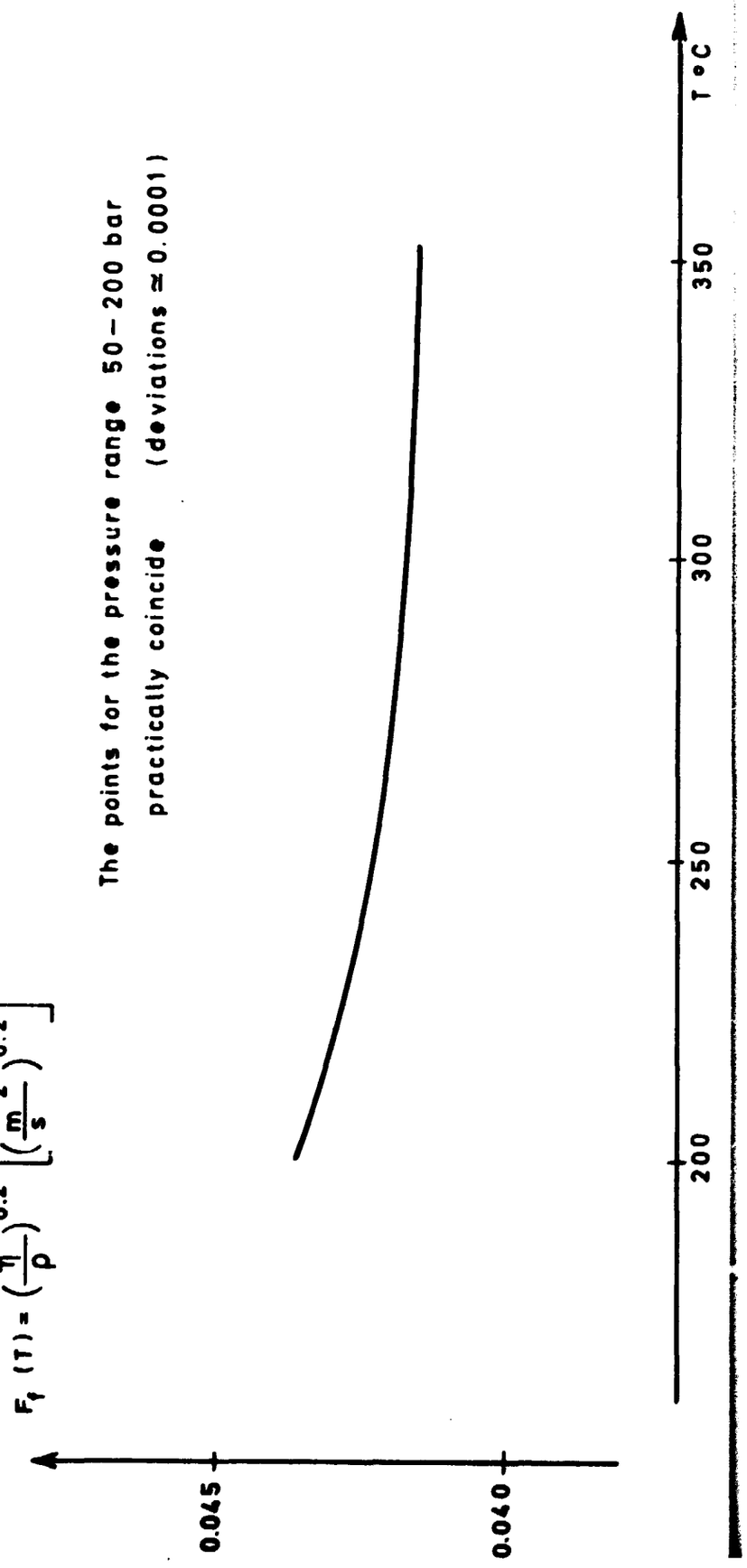




Fig. 12. The empirical relations $F_R$ and $F_\alpha$ for the simplified steam generator model.

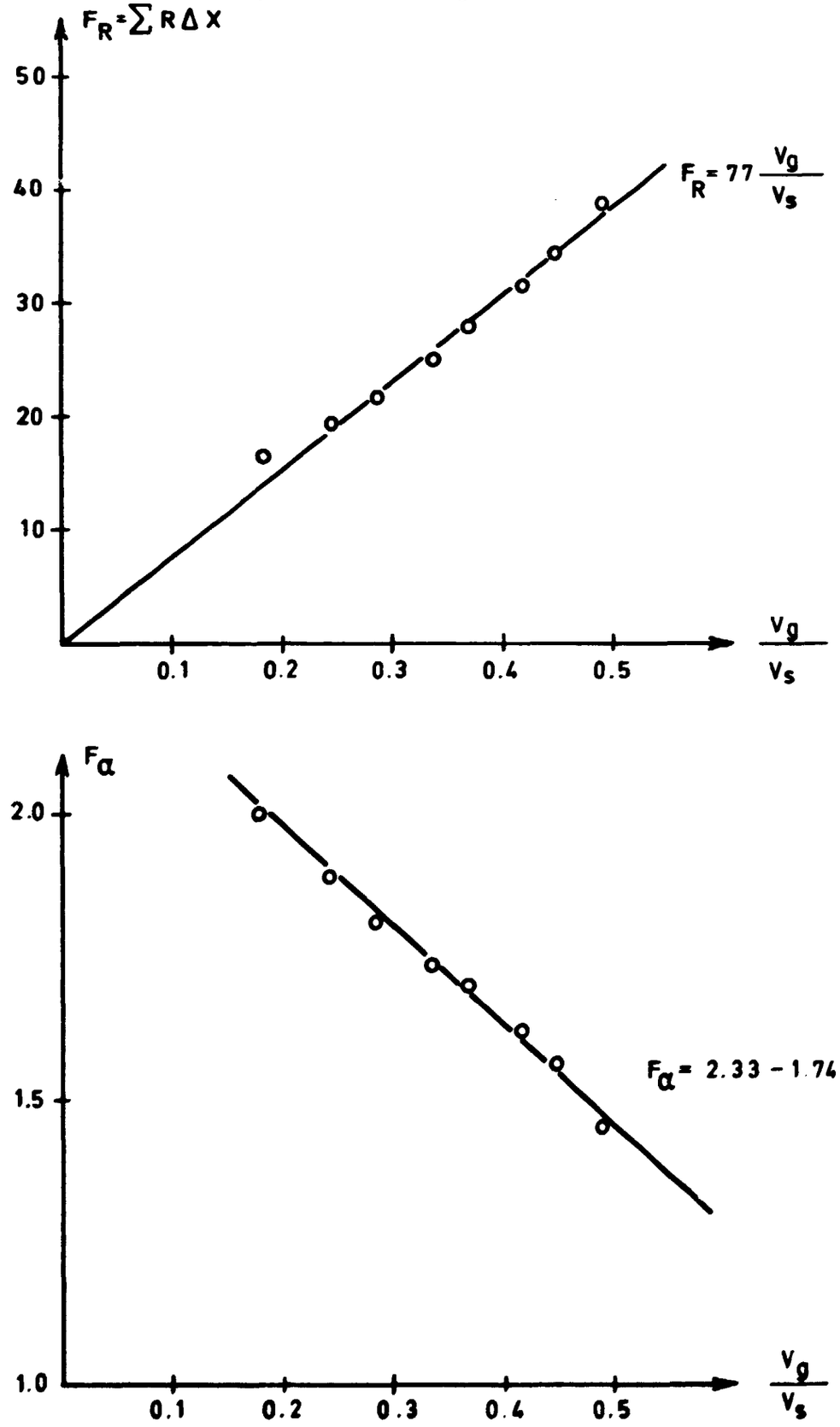

Fig. 13. Comparison of transient responses for the two steam generator models

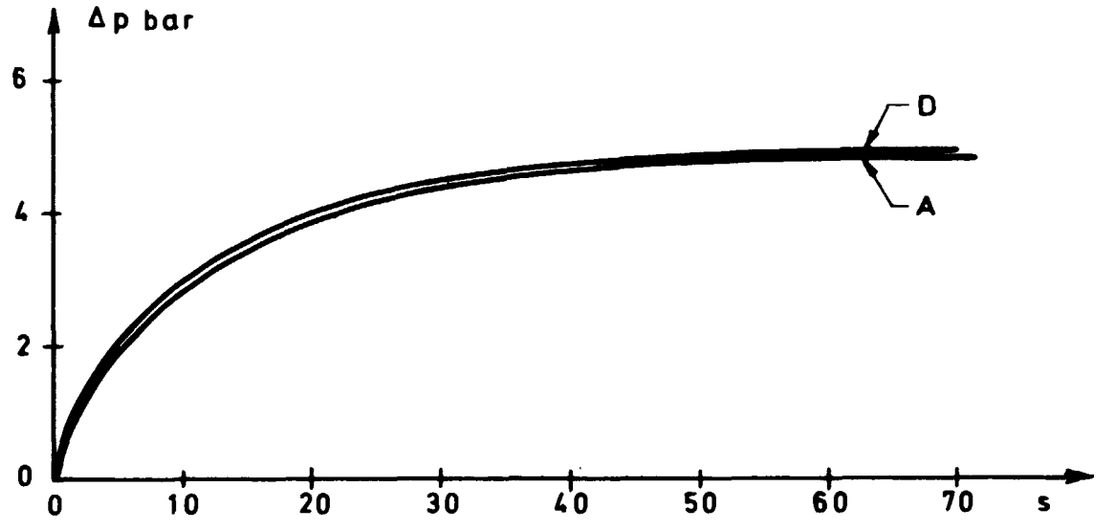


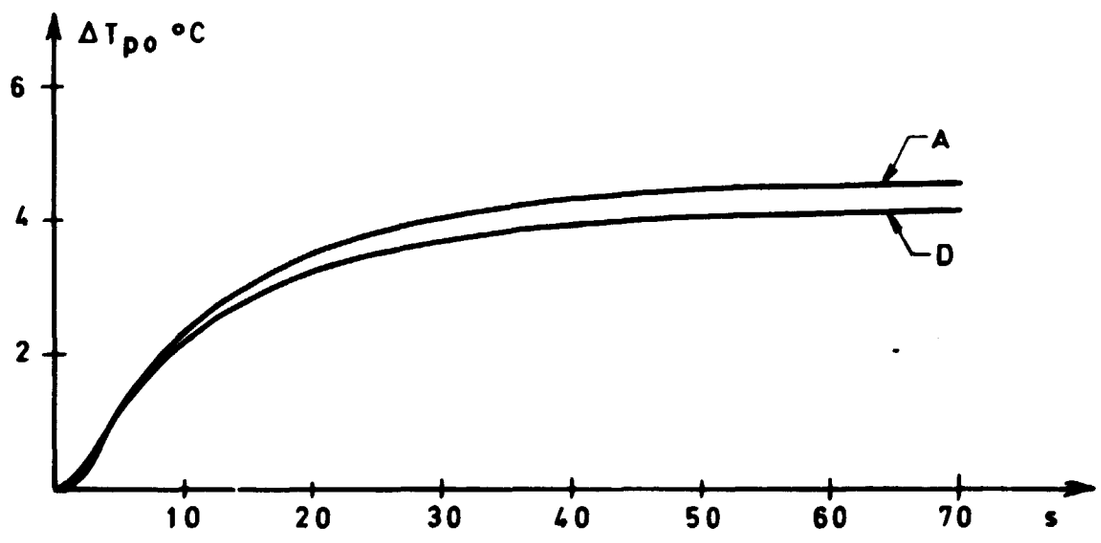


Transient responses of steam pressure and primary outlet temperature for a step in steam valve opening of -20 %

A : Simplified analog model

D : Detailed digital model



Fig. 14. Comparison of transient responses for the two steam generator models.

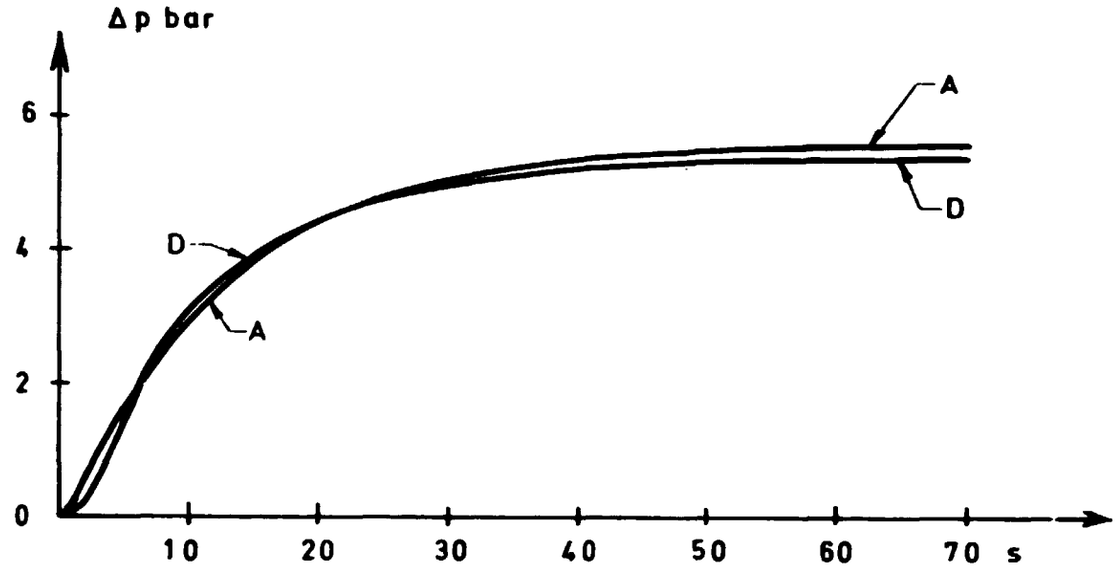


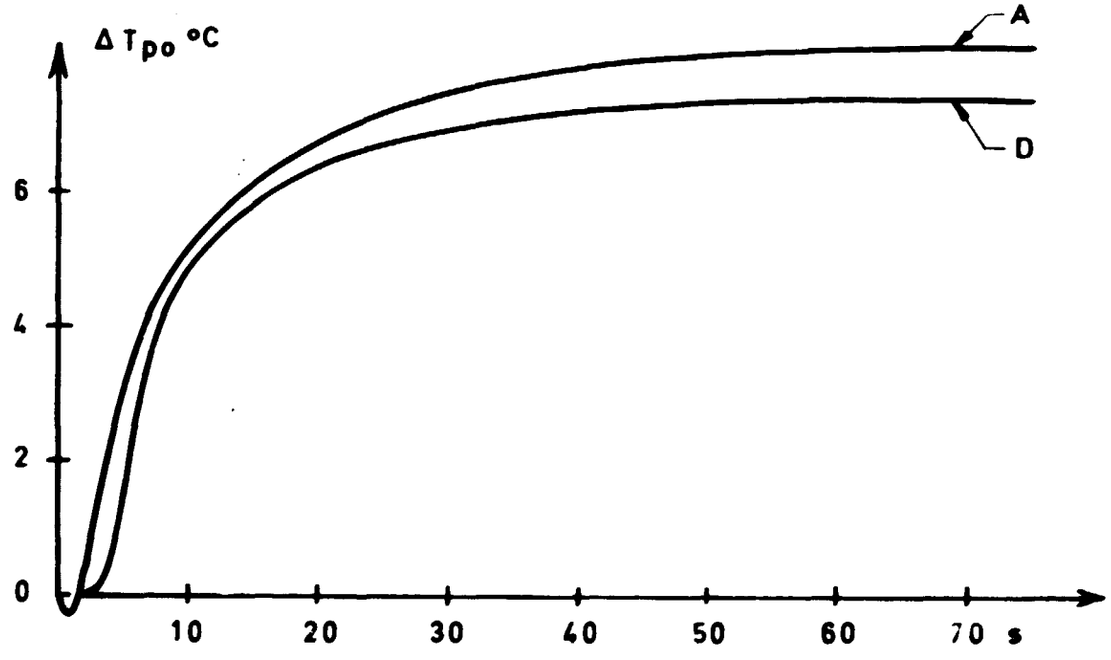


Transient responses of steam pressure and steam outlet temperature for a step in inlet temperature of +10 °C.

A : Simplified analog model.

D : Detailed digital model.

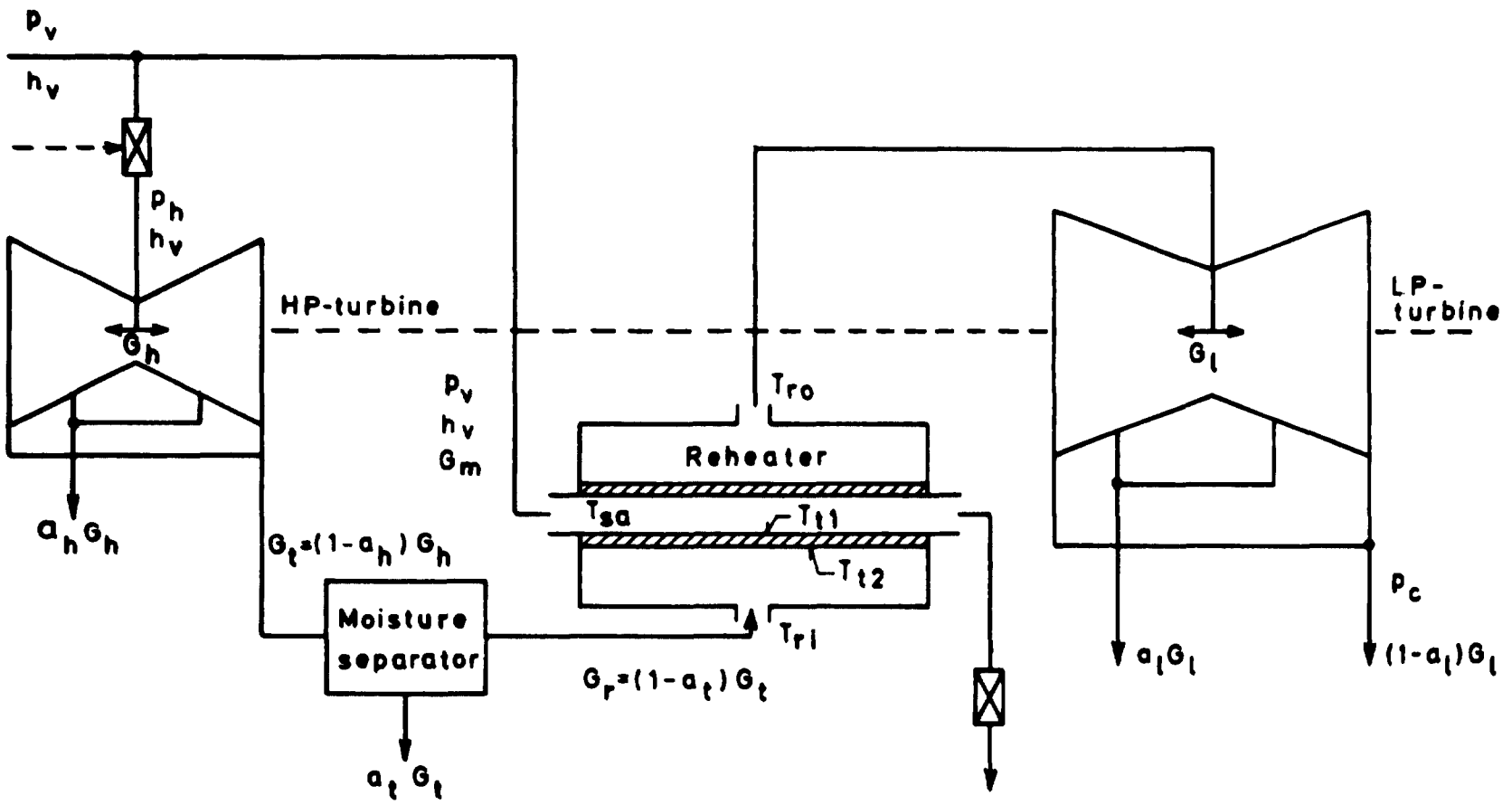


Fig. 15. Schematic flow diagram of turbine with moisture separator and reheater.



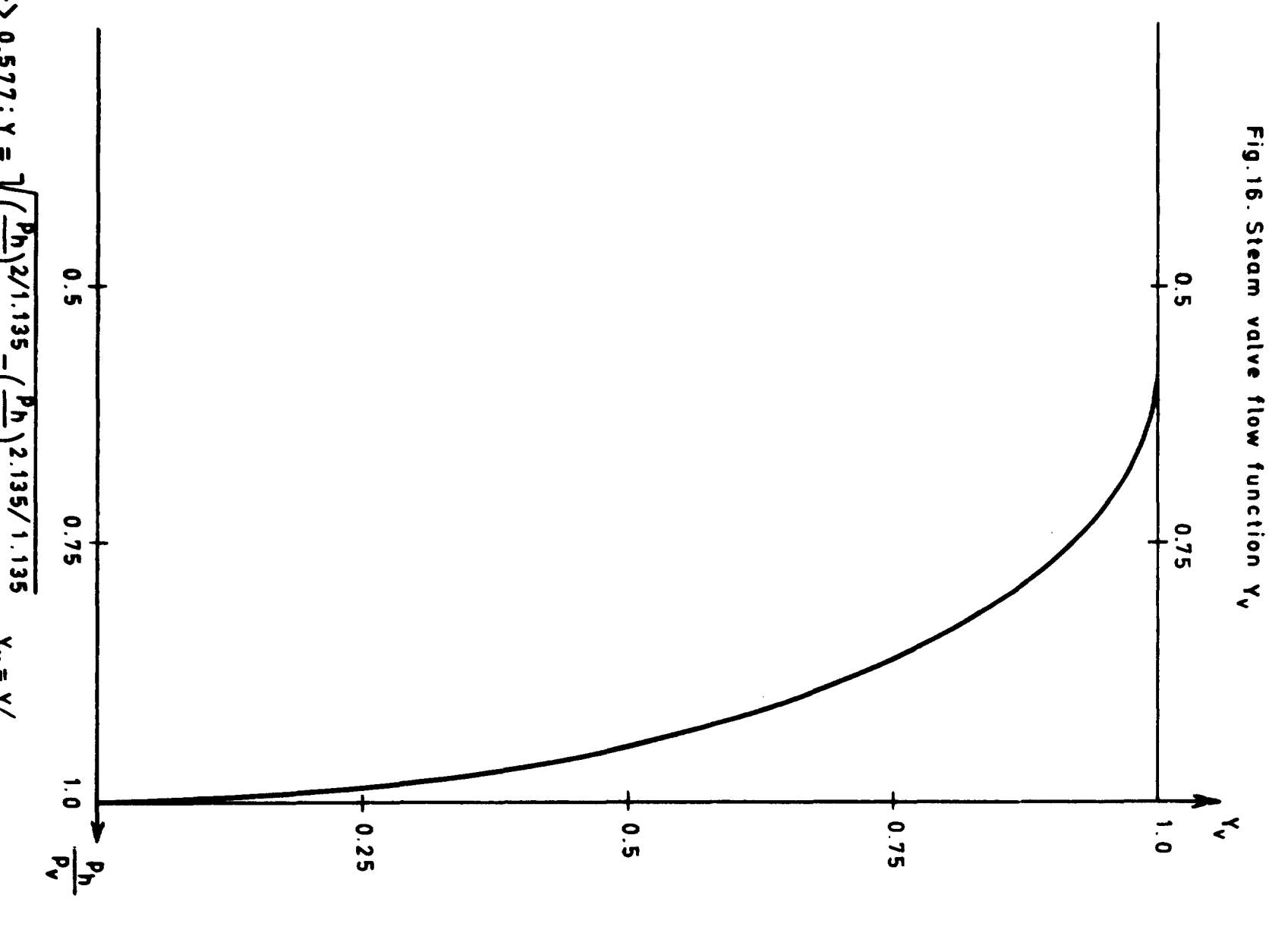


Fig. 16. Steam valve flow function $Y_v$

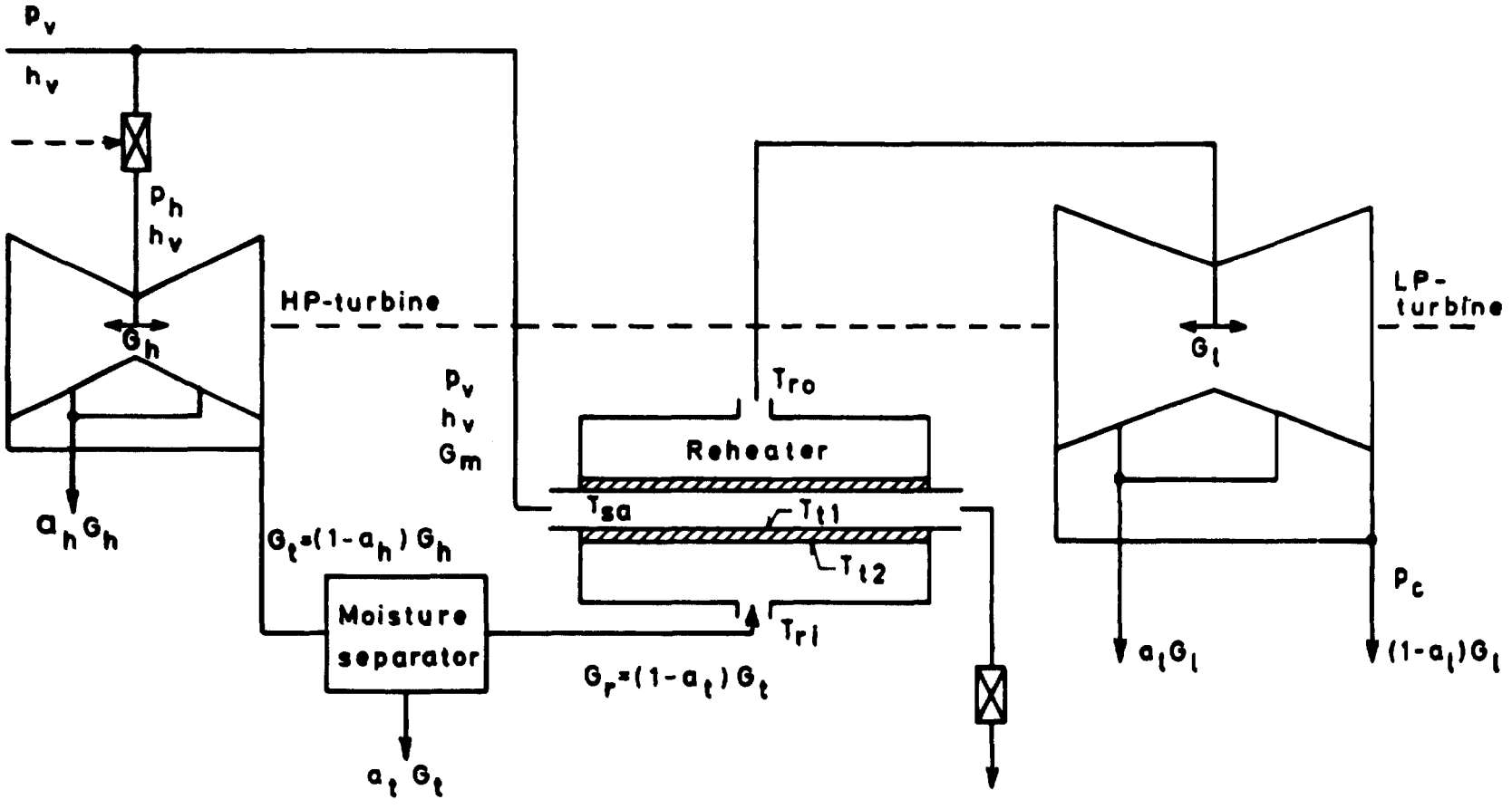


Fig. 15. Schematic flow diagram of turbine with moisture separator and reheater.



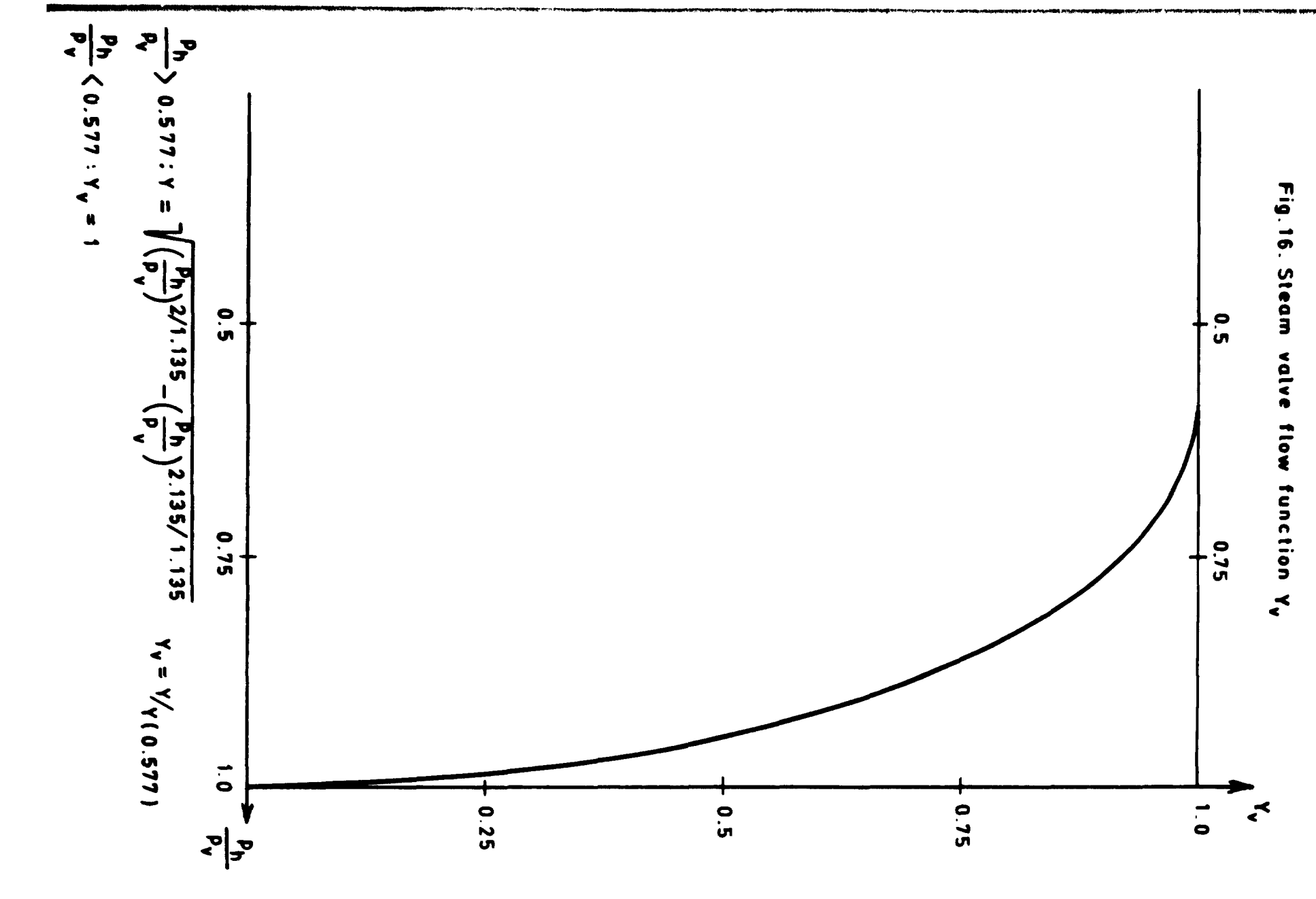


Fig. 16. Steam valve flow function $Y_v$